Improving crop yield prediction in Sweden using satellite remote sensing and the ecosystem model LPJ-GUESS

Li, Xueying

2025

LUND UNIVERSITY

PO Box 117
221 00 Lund
+46 46-222 00 00

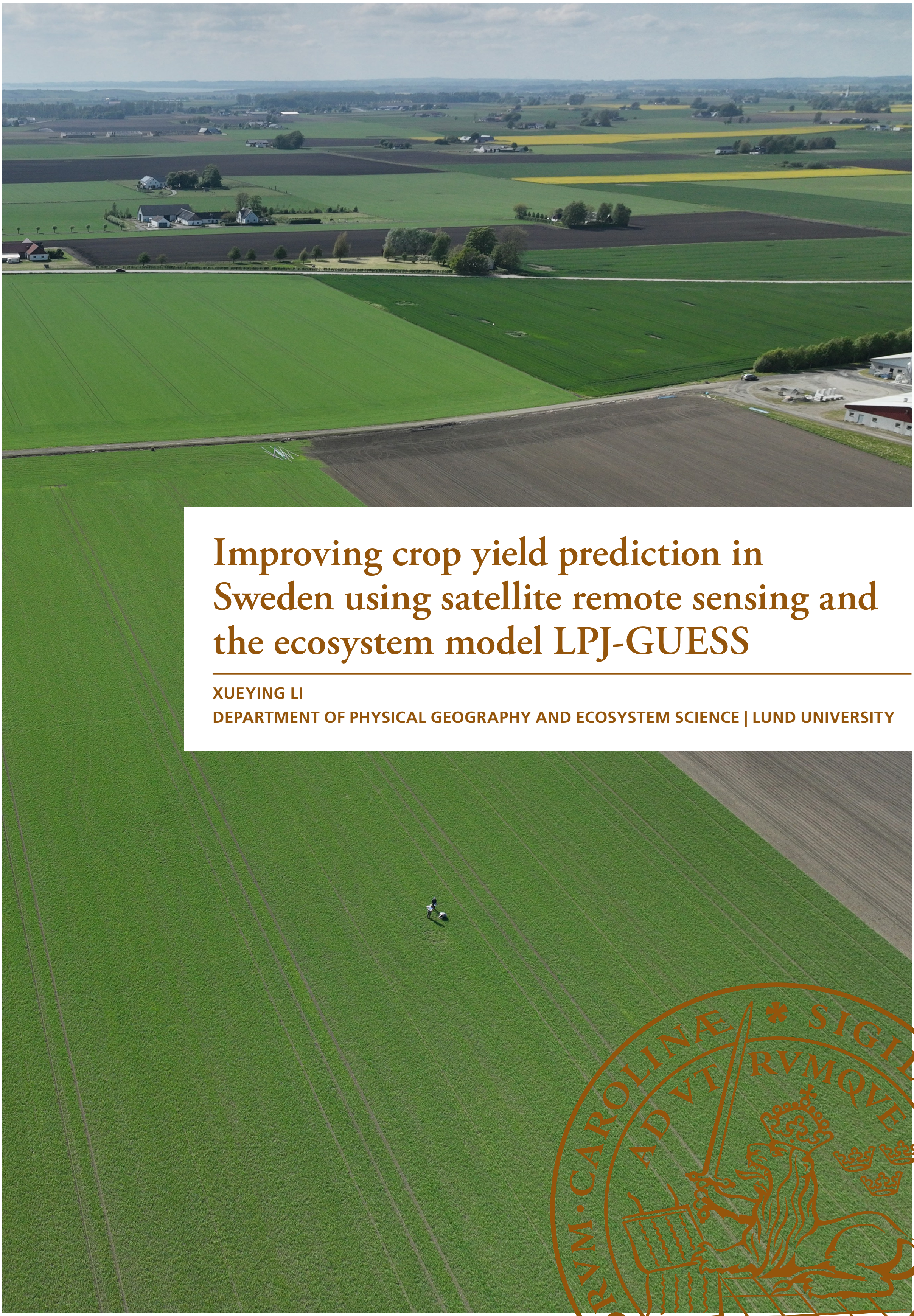

Improving crop yield prediction in Sweden using satellite remote sensing and the ecosystem model LPJ-GUESS

XUEYING LI
DEPARTMENT OF PHYSICAL GEOGRAPHY AND ECOSYSTEM SCIENCE | LUND UNIVERSITY

Printed by Media-Tryck, Lund 2025 NORDIC SWAN ECOLABEL 3041 0903

LUND UNIVERSITY

Faculty of Science
Department of Physical Geography
and Ecosystem Science

ISBN 978-91-89187-55-9

Improving crop yield prediction in Sweden using satellite remote sensing and the ecosystem model LPJ-GUESS

Improving crop yield prediction in Sweden using satellite remote sensing and the ecosystem model LPJ-GUESS

Xueying Li

LUND UNIVERSITY

DOCTORAL DISSERTATION

Doctoral dissertation for the degree of Doctor of Philosophy (PhD) at the Faculty of Science at Lund University to be publicly defended on date of 25th April at 09.00 AM in Pangea, Geocentrum II, Department of Physical Geography and Ecosystem Science, Sölvegatan 12, Lund

Faculty opponent
Professor Kaiyu Guan

Organization:

LUND UNIVERSITY
Department of Physical Geography and Ecosystem Science
Sölvegatan 12, SE-223 62 Lund, Sweden

Document name: DOCTORAL DISSERTATION

Date of issue: 2025-04-25

Author(s): Xueying Li

Sponsoring organization:

Title and subtitle: Improving crop yield prediction in Sweden using satellite remote sensing and the ecosystem model LPJ-GUESS

Abstract: Meeting the food demand of a growing global population with limited agricultural resources is one of the greatest challenges of the 21st century. Crop yield is highly sensitive to weather variability and climate extremes, which are becoming more frequent due to climate change. Accurate regional yield prediction is essential for helping farmers adapt, ensuring food security, and strengthening the resilience of agriculture. This PhD project focused on improving crop yield prediction in Sweden using satellite remote sensing and the ecosystem model LPJ-GUESS (Lund-Potsdam-Jena General Ecosystem Simulator), resulting in four research papers. Paper I introduced the first application of a triple collocation (TC)-based merging framework to evaluate the error structure of existing global evapotranspiration (ET) products and merge new ET datasets over the Nordic Region. The satellite-derived ET product Penman-Monteith-Leuning Version 2 (PML-V2) demonstrated the best overall performance among the selected ET products. Validated against Integrated Carbon Observation System (ICOS) in-situ measurements, the merged ET datasets outperformed individual parent products in terms of multiple evaluation metrics. This study provided reliable ET estimates to support the subsequent crop yield prediction. Paper II developed a novel framework for estimating spring barley yields at the district level in southern Sweden using meteorological data and multi-source satellite datasets with the random forest (RF) approach. The combination of vegetation indices (VIs) and solar-induced fluorescence (SIF) achieved high accuracy in crop yield estimation in April and May, suggesting that barley yield can be reliably forecasted two months prior to harvesting. Adding the monthly ET in June had slight contributions to the modelling performance. Paper III enhanced the performance of LPJ-GUESS (Lund-Potsdam-Jena General Ecosystem Simulator) in simulating district-level crop yields in southern Sweden by calibrating the model with observed yield and satellite-based ET data. Calibration with observed yield significantly improved accuracy for spring barley and winter wheat, while adding the satellite-based ET product PML-V2 led to only moderate gains. The calibrated model also effectively assessed the drought impacts of 2018, accurately estimating yield losses for both crops. Paper IV assessed the impacts of future climate change on crop yields in southern Sweden using the calibrated LPJ-GUESS model, driven by 3-km high-resolution climate projections. The results showed significant yield increases for spring barley and winter wheat by the end of the century under both Representative Concentration Pathways (RCP)4.5 and RCP8.5 scenarios. Rising carbon dioxide levels and warmer growing-season temperatures drove yield improvements, while reduced precipitation (i.e., drought) was expected to sharply decrease yields. This PhD project developed a robust framework for crop yield prediction using two approaches, following a state-of-the-art TC-based accuracy assessment of existing ET datasets. Our results provided a solid foundation for improving agricultural management in Sweden and supporting global efforts to enhance food security under climate change.

Key words: Evapotranspiration, Triple collocation; Crop yield prediction, Satellite remote sensing, Machine learning; Process-based crop models, Climate change

Language: English

Number of pages: 69

ISSN and key title:

ISBN (print): 978-91-89187-55-9
ISBN (PDF): 978-91-89187-56-6

Recipient's notes

Price

Security classification

Signature

Date 2025-03-14

Improving crop yield prediction in Sweden using satellite remote sensing and the ecosystem model LPJ-GUESS

Xueying Li

LUND
UNIVERSITY

Coverphoto by El Houssaine Bouras and back cover by Shangharsha Thapa

Faculty of Science

Department of Physical Geography and Ecosystem Science

ISBN (print): 978-91-89187-55-9

ISBN (PDF): 978-91-89187-56-6

Printed in Sweden by Media-Tryck, Lund University

Lund 2025

NORDIC SWAN ECOLABEL
Printed matter
3041 0903

Media-Tryck is a Nordic Swan Ecolabel certified provider of printed material. Read more about our environmental work at www.mediatryck.lu.se

MADE IN SWEDEN

To Vimukthi

Table of Contents

Abstract

Meeting the food demand of a growing global population with limited agricultural resources is one of the greatest challenges of the 21st century. Crop yield is highly sensitive to weather variability and climate extremes, which are becoming more frequent due to climate change. Accurate regional yield prediction is essential for helping farmers adapt, ensuring food security, and strengthening the resilience of agriculture. This PhD project focused on improving crop yield prediction in Sweden using satellite remote sensing and the ecosystem model LPJ-GUESS (Lund-Potsdam-Jena General Ecosystem Simulator), resulting in four research papers. Paper I introduced the first application of a triple collocation (TC)-based merging framework to evaluate the error structure of existing global evapotranspiration (ET) products and merge new ET datasets over the Nordic Region. The satellite-derived ET product Penman-Monteith-Leuning Version 2 (PML-V2) demonstrated the best overall performance among the selected ET products. Validated against Integrated Carbon Observation System (ICOS) in-situ measurements, the merged ET datasets outperformed individual parent products in terms of multiple evaluation metrics. This study provided reliable ET estimates to support the subsequent crop yield prediction. Paper II developed a novel framework for estimating spring barley yields at the district level in southern Sweden using meteorological data and multi-source satellite datasets with the random forest (RF) approach. The combination of vegetation indices (VIs) and solar-induced fluorescence (SIF) achieved high accuracy in crop yield estimation in April and May, suggesting that barley yield can be reliably forecasted two months prior to harvesting. Adding the monthly ET in June had slight contributions to the modelling performance. Paper III enhanced the performance of LPJ-GUESS (Lund-Potsdam-Jena General Ecosystem Simulator) in simulating district-level crop yields in southern Sweden by calibrating the model with observed yield and satellite-based ET data. Calibration with observed yield significantly improved accuracy for spring barley and winter wheat, while adding the satellite-based ET product PML-V2 led to only moderate gains. The calibrated model also effectively assessed the drought impacts of 2018, accurately estimating yield losses for both crops. Paper IV assessed the impacts of future climate change on crop yields in southern Sweden using the calibrated LPJ-GUESS model, driven by 3-km high-resolution climate projections. The results showed significant yield increases for spring barley and winter wheat by the end of the century under both Representative Concentration Pathways (RCP)4.5 and RCP8.5 scenarios. Rising carbon dioxide levels and warmer growing-season temperatures drove yield improvements, while reduced precipitation (i.e., drought) was expected to sharply decrease yields. This PhD project developed a robust framework for crop yield prediction using two approaches, following a state-of-the-art TC-based accuracy assessment of existing ET datasets. Our results provided a solid foundation for improving agricultural management in Sweden and supporting global efforts to enhance food security under climate change.

Popular summary

Meeting the growing demand for food driven by a rapidly expanding global population is one of the most pressing challenges of the 21st century. Crop yield, which measures the amount of harvest produced relative to the land area used for cultivation, is a key indicator of agricultural productivity. Accurate predictions of crop yields help farmers optimize their financial planning and farming strategies, while also playing a crucial role in preventing food shortages and ensuring global food security. Most previous research on crop yield prediction falls into two categories: data-driven, satellite-based empirical models and process-based crop models. This PhD project aimed to improve crop yield predictions in Sweden by leveraging both approaches, providing a more comprehensive and reliable understanding of future food production from multiple perspectives.

The development of high-quality evapotranspiration (ET) products is essential for enhancing the accuracy of crop yield predictions. As such, the first part of this project involved evaluating the accuracy of several existing ET datasets in the Nordic Region. The datasets with the least error were selected for further research. The second part of this project focused on predicting spring barley yield using satellite remote sensing data, climate information, and machine learning techniques. The results demonstrated that satellite-based vegetation indices (VIs) and solar-induced fluorescence (SIF) could achieve high accuracy in crop yield estimation during April and May. This suggested that the model could predict spring barley yields up to two months before harvest. The third part of the project aimed to improve crop yield simulations in the process-based ecosystem model LPJ-GUESS (Lund-Potsdam-Jena General Ecosystem Simulator). Six parameters related to crop growth in LPJ-GUESS were modified to better simulate crop yields in southern Sweden. By fine-tuning the model with real-world yield data and satellite-based ET datasets, the model's ability to predict the yields of spring barley and winter wheat improved, particularly during extreme weather events like the drought in 2018. The final part of this project explored how climate change might impact crop yields in southern Sweden under different climate scenarios by using the calibrated LPJ-GUESS from the last work. The results indicated significant yield increases for both spring barley and winter wheat by the end of the century. Warmer temperatures and higher carbon dioxide levels were found to generally boost yields, although drought conditions could lead to sharp declines in production. From the methodological perspective, this project developed an effective framework to improve the accuracy of crop yield prediction in Sweden using both satellite remote sensing data and the ecosystem LPJ-GUESS model, which can also be applied to other crops and regions. From the knowledge perspective, all these studies provided powerful instructions to enhance agricultural management and safeguard food security in a changing climate. We hope the outcome of this project will enable farmers and policymakers to make smarter, more informed decisions.

Populärvetenskaplig sammanfattning

Förmågan att möta växande efterfrågan på mat, driven av en snabbt expanderande global befolkning, är en av våra mest pressande utmaningar under det kommande århundradet. Skördeutbyte, som mäter mängden skörd i förhållande till den odlade ytan, är en nyckelindikator för jordbrukets produktivitet. Noggrannare prognoser för skördeutbyte hjälper lantbrukare att optimera sin ekonomiska planering och sina jordbruksstrategier, samtidigt som de spelar en avgörande roll för att förhindra livsmedelsbrist och säkerställa global livsmedelsförsörjning.

En majoritet av de tidigare forskningsarbeten som involverar skördeutbytesprognoser kan oftast delas in i två olika metodkategorier: antingen använder de sig främst av datadrivna, satellitbaserade empiriska modeller eller så använder de sig av processbaserade växtmodeller. Denna avhandling syftar till att förbättra prognoser för skördeutbyte i Sverige genom att använda sig av en kombination av båda dessa tillvägagångssätt. Detta syftar till att ge en mer omfattande och tillförlitlig förståelse till framtida livsmedelsproduktion utifrån olika perspektiv.

Högkvalitativa evapotranspirations-(ET) dataprodukter är avgörande för att förbättra noggrannheten i skördeutbytesprognoser. Därför handlar den första delen av avhandlingen om att utvärdera noggrannheten hos flera befintliga ET-dataprodukter i den nordiska regionen. De ET-dataprodukter som uppvisade bäst resultat i detta steg valdes ut för vidare forskning. Den andra delen av projektet fokuserade vidare på att uppskatta skördeutbyte av vårkorn med hjälp av satellitbaserade fjärranalysdata, klimatvariabler och maskininlärningstekniker. Resultaten visade att användandet av satellitbaserade vegetationsindex (VIs) och solinducerad fluorescens (SIF) kunde bidra till att uppnå en hög noggrannhet vid skördeutbytesuppskattning redan i april och maj. Detta tyder på att modellen kan förutsäga vårkornets skördeutbyte upp till två månader innan skörden. Den tredje delen av projektet syftade till att förbättra skördeutbytesimuleringarna i den processbaserade ekosystemmodellen LPJ-GUESS (Lund-Potsdam-Jena General Ecosystem Simulator). Sex parametrar relaterade till växttillväxt i LPJ-GUESS modifierades för att bättre simulera skördeutbyten i södra Sverige. Genom att finjustera modellen med verkliga skördeobservationer och satellitbaserade ET-dataprodukter, förbättrades modellens förmåga att förutsäga skörden av vårkorn och vintervete, särskilt gällde detta under extrema väderhändelser, exempelvis sommartorkan 2018. I den avslutande delen av projektet utforskades hur klimatförändringar kan påverka skördeutbyte i södra Sverige under olika klimatscenarier med hjälp av den kalibrerade LPJ-GUESS-modellen, som kalibrerades i den föregående delen av projektet. Resultaten här indikerar betydande ökningar av skördeutbyte för både vårkorn och vintervete vid seklets slut. Varmare temperaturer och högre koldioxidnivåer som väntas råda i framtiden visade sig generellt öka skörden, även om torkförhållanden kan leda till kraftiga minskningar i produktionen. Utifrån ett metodologiskt perspektiv utvecklade detta projekt en effektiv ram för att förbättra noggrannheten i skördeutbudsprognoser i Sverige genom att använda både satellitbaserade fjärranalysdata och ekosystemmodellen LPJ-GUESS, vilket också kan tillämpas på andra grödor och regioner. Från ett kunskapsperspektiv gav dessa studier kraftfulla verktyg för att förbättra jordbrukshantering och säkerställa framtida livsmedelsförsörjning i ett förändrat klimat. Vi hoppas därmed att resultatet av detta projekt kommer att kunna hjälpa lantbrukare och beslutsfattare att fatta smartare och mer informerade beslut.

List of papers

Paper I
Li, X., Zhang, W., Vermeulen, A., Dong, J., Duan, Z. (2023). Triple collocation-based merging of multi-source gridded evapotranspiration data in the Nordic Region. *Agricultural and Forest Meteorology*, 335, 109451.

Paper II
Li, X., Jin, H., Eklundh, L., Bouras, E., Olsson, P., Cai, Z., Ardö, J., Duan, Z. (2024). Estimation of district-level spring barley yield in southern Sweden using multi-source satellite data and random forest approach. *International Journal of Applied Earth Observation and Geoinformation*, 134, 104183.

Paper III
Li, X., Zhang, W., Wu, M., Olin, S., Zhou, H., Huang, X., Thapa, S., Bouras, E., Duan, Z. Calibrating the dynamic vegetation model LPJ-GUESS for crop yield simulation in southern Sweden using satellite-based evapotranspiration data and observed crop yield. (*Manuscript submitted to Field Crops Research*)

Paper IV
Li, X., Wu, M., Zhang, W., Huang, X., Lind, P., Duan, Z. Assessing climate change impacts on crop yields in southern Sweden using the ecosystem model LPJ-GUESS with the convection-permitting regional climate data. (*Manuscript in preparation*)

Published papers during the doctoral program not included in this thesis

Li, X., Zhu, W., Xie, Z., Zhan, P., Huang, X., Sun, L., Duan, Z. (2021). Assessing the effects of time interpolation of NDVI composites on phenology trend estimation. *Remote Sensing*, 13(24), 5018.

Wei, L., Jiang, S., Dong, J., Ren, L., Yong, B., Yang B., **Li, X.,** Duan, Z. (2024). A combined extended triple collocation and cumulative distribution function merging framework for improved daily precipitation estimates over mainland China. *Journal of Hydrology*, 641, 131757.

Author’s contribution to the papers

Paper I
Xueying Li: Methodology, Data curation, Data analysis, Visualization, Validation, Discussion, Writing – original draft. Wenxin Zhang: Discussion, Co-supervision, Writing – review & editing. Alex Vermeulen: Writing – review & editing. Jianzhi Dong: Methodology, Data analysis, Discussion, Writing – review & editing. Zheng Duan: Conceptualization, Methodology, Data analysis, Discussion, Supervision, Writing – review & editing, Funding acquisition.

Paper II
Xueying Li: Data curation, Formal analysis, Methodology, Software, Validation, Writing – original draft, Writing – review & editing. Hongxiao Jin: Writing – review & editing. Lars Eklundh: Writing – review & editing. El Houssaine Bouras: Methodology, Writing – review & editing. Per-Ola Olsson: Writing – review & editing. Zhanzhang Cai: Data Curation, Writing – review & editing. Jonas Ardö: Writing – review & editing. Zheng Duan: Conceptualization, Funding acquisition, Methodology, Project administration, Supervision, Writing – review & editing.

Paper III
Xueying Li: Data curation, Formal analysis, Methodology, Software, Validation, Writing – original draft, Writing – review & editing. Wenxin Zhang: Data curation, Formal analysis, Methodology, Software, Writing – review & editing. Minchao Wu: Methodology, Software, Writing – review & editing. Stefan Olin: Methodology, Software. Hao Zhou: Software, Writing – review & editing. Xin Huang: Formal analysis, Writing – review & editing. Shangharsha Thapa: Writing – review & editing. El Houssaine Bouras: Writing – review & editing. Zheng Duan: Conceptualization, Funding acquisition, Methodology, Project administration, Supervision, Writing – review & editing.

Paper IV
Xueying Li: Data curation, Formal analysis, Methodology, Software, Validation, Writing – original draft, Writing – review & editing. Minchao Wu: Data curation, Formal analysis, Methodology, Software, Writing – review & editing. Wenxin Zhang: Data curation, Software, Writing – review & editing. Xin Huang: Formal analysis, Writing – review & editing. Petter Lind: Data curation, Writing – review & editing. Zheng Duan: Conceptualization, Funding acquisition, Methodology, Project administration, Supervision, Writing – review & editing.

Abbreviations

C	Carbon
CMIP	Coupled Model Intercomparison Project
CPRCMs	Convection-permitting regional climate models
CRO	Cropland
CO_2	Carbon dioxide
DS	Developmental stage
EC	Eddy Covariance
ECC	Error cross-correlation
ECMs	Earth System Models
ENF	Evergreen needleleaf forest
ET	Evapotranspiration
ETC	Extended Triple Collocation
GCMs	General Circulation Models
GLEAM	Global Land Evaporation Amsterdam Model
ICOS	Integrated Carbon Observation System
LAI	Leaf Area Index
LC	End-of-century
LPJ-GUESS	Lund-Potsdam-Jena General Ecosystem Simulator
MAE	Mean Absolute Error
MC	Mid-century
MF	Mixed forest
N	Nitrogen
NDVI	Normalized Difference Vegetation Index
nRMSE	Normalized Root Mean Squared Error
PML-V2	Penman-Monteith-Leuning Version 2
PPI	Plant Phenology Index
QC	Quadruple collocation
QM	Quantile mapping

RCP	Representative Concentration Pathways
RF	Random forest
RMSE	Root Mean Squared Error
SB	Spring barley
SBF	Sparse boreal forest
SIF	Solar-induced fluorescence
TC	Triple collocation
ubRMSE	Unbiased Root Mean Squared Error
VIs	Vegetation indices
WW	Winter wheat

Acknowledgements

Completing my PhD would not have been possible without the guidance, support, and care of many wonderful people who have accompanied me on this journey. I am deeply grateful to everyone who has joined me along the way.

First and foremost, I am sincerely grateful to my supervisors, Zheng and Wenxin. Being chosen for this PhD position has truly changed the course of my life. Thank you for your timely feedback, detailed guidance, and endless patience over the past four years. You have not only cultivated my research abilities but also sparked a deep interest in my work. Beyond being mentors, you are also like friends. I truly appreciate both of you sharing career experiences, as well as offering invaluable advice for my own life. This work would not have been possible without your support. I hope that my four years of achievements meets your expectations and brings you satisfaction. I am also grateful to Andreas, my department representative, who provided annual academic support and consistently showed concern for my research plans, study environment, and well-being throughout my PhD.

I would like to acknowledge my other co-authors—Alex, El Houssaine, Hao, Hongxiao, Jianzhi, Jonas, Lars, Minchao, Per-Ola, Petter, Shangharsha, Stefan, Xin, and Zhanzhang—for your invaluable contributions to the papers and the thoughtful discussions during writing the response letters. It has been a pleasure to collaborate with all of you, bringing together such a wide range of skills.

For all my colleagues and staff in INES, I extend my heartfelt gratitude. Thank you for the help from Camilla, Christina, Ekaterina, Gisela, Irma, Ricki, Yvonne in CGB-kansli, and for the technical support from Rafael, Rebecca, and Ricardo. A special thanks to my fellow PhD colleagues, for all the lovely moments we spent together. Thank you to Anna, Anna-Kristina, Antje, Aleksander, Alexandra, Akash, Arti, Babak, Camille, Carlos, Chansopheaktra, Deborah, Didac, Emily, Filipe, Gilbert, Hanna, Hani, Hao, Haoming, Jalisha, Jiahui, John, Karolina, Kimberly, Lovisa, Margot, Mayra, Mitro, Pheaktra, Qin, Renkui, Ross, Shangharsha, Shubham, Tristan, Wan Ni, Veronika, Yuzuo, and all the other PhD colleagues past and present. Thank you as well to everyone I have not mentioned by name. Each of you has contributed to creating a warm and supportive environment in INES, offering me care and encouragement throughout my PhD journey.

I would also like to express my deepest gratitude to my family—my parents, grandparents, and aunt—for their unwavering financial and emotional support throughout my educational journey. My grandmother, born in a remote rural area, was one of the few women in her village to rise above her circumstances through education. Due to the severe poverty, her younger brother sacrificed his own right to an education at the age of twelve to ensure that my grandmother could continue her studies. Without his selflessness and my grandmother's perseverance, my own

life path would have been entirely different. I offer my highest respect to them both. Following in my grandmother's footsteps, my mother excelled in school, earning top grades and securing a place at universities in a larger city. They have always understood the transformative power of education—especially for women—and have fully supported my pursuit of a higher degree. It is because of their vision and tireless efforts across two generations that I have been able to experience a broader world and live a life they never had the chance to. I am incredibly fortunate to have been born into such a remarkable family. I hope this work makes them proud.

To my husband, Vimukthi — my other half. We have been by each other's side for nearly a decade, and choosing to spend my life with you is the best decision I have ever made. You are my chef, driver, therapist, gym partner, travel companion, and my best friend. Together, we share life's joys and sorrows, make important decisions, and support each other wholeheartedly through every step. Being with you gives me endless strength and motivation to keep progressing. With your care and love, I am always confident to become the best version of myself. You are my lucky charm.

Lastly, I want to thank myself. Four years ago, I packed my future into two large suitcases and arrived in Lund on a winter night—my very first time in Europe. Over the past years, I've learned to adapt to a new environment, overcome language barriers, attempt to learn Swedish, and explore various research areas. Completing this PhD journey has been like an adventure, revealing to me that I am brave and capable enough to begin the next chapter of my life. No matter what comes my way, I believe I can face it, handle it, and move forward. I am hopeful for the bright future ahead.

Introduction

The importance of crop yield prediction under climate change

Global food security is under increasing pressure as the world population continues to rise. The 2020 World Population Data Sheet from the Population Reference Bureau projected a continuous increase in the global population from 7.8 billion in 2020 to 9.9 billion by 2050. Meeting the resulting food demand would require a 25%–70% increase in current crop production levels (Hunter et al., 2017). Ensuring food security under rapid population growth remains one of the most critical challenges of the 21st century (Godfray et al., 2010). Crop yield, defined as the ratio of harvested product to the cropped area (Carletto et al., 2015), is a fundamental measure of food productivity. Crop yields are highly sensitive to weather variability and climate extremes (Osborne et al., 2007). Climate change, driven by rising temperatures and increased atmospheric carbon dioxide (CO_2) levels, significantly affects the thermal growing seasons of plants, including their quantity and duration (Easterling et al., 2007). It also alters soil conditions, such as nutrient availability, soil temperature, and moisture, while impacting key agricultural management strategies essential for sustainable crop production (Gomez-Zavaglia et al., 2020). Additionally, human-induced climate change has increased the frequency and intensity of daily temperature and precipitation extremes (Zhang et al., 2013), leading to extreme events such as floods, droughts, and wildfires worldwide (Schickhoff et al., 2016), posing significant challenges to global food security. In 2018, northern Europe experienced widespread and simultaneous crop yield reduction due to an unusual combination of exceptionally low rainfall and high temperature from March to August (Beillouin et al., 2020). In Sweden, grain production declined by 45% compared to 2017, marking a 43% decrease from the five-year average and the lowest yield recorded in 59 years (Statistiska Meddelanden, 2018). These events highlight the urgent need to improve our understanding of climate change impacts on crop production, which is essential for developing effective adaptation strategies to enhance the resilience of the agricultural sector in a changing climate.

Accuracy assessment of multi-source ET data for crop yield prediction

Terrestrial evapotranspiration (ET) represents the total loss of water through canopy interception, plant transpiration, and soil evaporation (Samuel et al., 2018). Given its critical role in the plant physiological processes, ET serves as an essential variable for monitoring and estimating the agricultural production (Tadesse et al., 2015; Yang et al., 2018). Therefore, the development of high-quality ET products is crucial for improving the accuracy of crop yield prediction.

In recent decades, multiple global gridded ET products have been developed, primarily driven by three approaches: (1) remote sensing-based approach, including the Global Land Evaporation Amsterdam Model (GLEAM) (Miralles et al., 2011), MOD16 (Mu et al., 2007), and the Priestley-Taylor Jet Propulsion Laboratory algorithm (Fisher et al., 2008); (2) model-based approach, such as the Medium-Range Weather Forecasts model (Crow et al., 2020), ERA-5 (Hersbach et al., 2020), the Global Land Data Assimilation System (Rodell et al., 2004), the Land Surface Analysis-Satellite Application Facility model (Ghilain et al., 2011), and the Mapping Evapotranspiration with Internalized Calibration model (Allen et al., 2007); and (3) upscaling or interpolation of in situ measurements, exemplified by FLUXCOM (Jung et al., 2019). However, each ET estimation method is subject to distinct sources of uncertainty, including sensor calibration limitations (Jia et al., 2012), model parameterization challenges (Byun et al., 2014), and errors in in situ observations (Baik et al., 2016). These uncertainties highlight the need for robust error estimation techniques to assess and improve the accuracy of ET products.

Eddy Covariance (EC) systems have been widely utilized to measure latent heat fluxes—the energy-driving ET—and are commonly regarded as the "ground truth" for evaluating ET estimates. Frequently used EC measurement networks include AmeriFlux (Yang et al., 2021), LaThuileFlux and AsiaFlux (Yao et al., 2015), the FLUXNET Canada Research Network (Wang et al., 2015), the Coordinated Enhanced Observing Period and ChinaFLUX (Yao et al., 2013), and the Southern African Regional Science Initiative (SAFARI 2000) project (Majozi et al., 2017). However, EC-based evaluations pose challenges in regions with limited or no available EC measurement sites. In the Nordic Region, which serves as the study area for this research, only a small number of EC stations are available for validating ET products. For instance, FLUXCOM includes latent heat data from eight sites (Tramontana et al., 2016), GLEAM relies on only two sites (Martens et al., 2017), and Penman-Monteith-Leuning Version 2 (PML-V2) incorporates data from three sites (Zhang et al., 2019). The scarcity of measurement sites in this region complicates efforts to achieve reliable ET product validation.

Triple collocation (TC) analysis (Stoffelen, 1998) is a widely used statistical approach for quantifying uncertainties in various geophysical products. This method has been extensively applied to assess errors in datasets related to precipitation (Dong et al., 2020; Duan et al., 2021), soil moisture (Chen et al., 2018; Xu et al., 2021), and ocean wind speed and wave height products (Li et al., 2021). Unlike traditional validation methods that rely on ground observations, TC enables the evaluation of dataset uncertainties across broader geographic regions (Chen et al., 2021). The TC technique estimates the uncertainty (i.e., error variance) of input datasets within a triplet without requiring knowledge of the absolute truth. Building on this methodology, Yilmaz et al. (2012) developed a TC-based least squares merging approach to generate improved products by integrating multiple parent datasets. McColl et al. (2014) extended the TC framework by introducing Extended Triple Collocation (ETC), which calculates the correlation of geophysical products with an unknown true state. Despite the versatility of TC, its application to ET products remains limited (Khan et al., 2018). No existing studies have specifically examined ET product uncertainties and developed merged ET datasets in the Nordic Region.

Main crop yield prediction approaches

Two primary approaches have been developed in recent decades to enhance the timeliness and spatial coverage of crop yield prediction: (1) satellite-based empirical models and (2) process-based crop growth models, with a specific focus here on the ecosystem model LPJ-GUESS (Lund-Potsdam-Jena General Ecosystem Simulator). Satellite-based empirical models, some combined with machine learning techniques, rely on the observed remote sensing data to predict crop yield within the current or upcoming growing season, provided that relevant satellite-based environmental variables are available. On the other hand, process-based crop growth models, such as LPJ-GUESS, can be driven by climate projections to enable longer-term climate impact assessment. By estimating plant-climate interactions and simulating biophysical processes, both models offer valuable insights into future agricultural productivity under varying climatic conditions. As crop yield prediction using LPJ-GUESS relies on future climate data, this chapter focuses on introducing the model itself. The climate data and the application of the model for crop yield prediction are addressed in the subsequent chapter.

Satellite-based empirical models

Satellite-based empirical models involve the establishment of statistical relationships between in-situ crop yield data and satellite-derived variables. The rapid advancement of satellite remote sensing technology has significantly enhanced the potential for accurate and reliable crop yield estimates in regional studies (Tucker et al., 1981; Murthy et al., 1996; Wardlow and Egbert, 2008;

Mariotto et al., 2013; Azzari et al., 2017; Mateo-Sanchis et al., 2019; Marshall et al., 2022). Currently, three primary satellite-derived variables are commonly used for estimating crop production: (1) vegetation indices (VIs), (2) biophysical or biochemical features, and (3) abiotic factors (Moulin et al., 1998; Johnson, 2014; Marshall et al., 2022).

Commonly used VIs were derived from surface reflectance measurements, primarily in the red and near-infrared wavelengths from satellite observations (Lobell, 2013). The widely applied VIs include the Normalized Difference Vegetation Index (NDVI, James and Kalluri, 1994), Enhanced Vegetation Index (Huete et al., 2002), Difference Vegetation Index (Richardson and Wiegand, 1977), Soil Adjusted Vegetation Index (Huete, 1988), and the recently introduced Plant Phenology Index (PPI, Jin and Eklundh, 2014). A typical biophysical feature used in crop yield estimation is the Leaf Area Index (LAI), which represents half of the total green leaf area per unit of horizontal ground surface area (Chen and Black, 1992). Another significant biochemical proxy is Solar-Induced Fluorescence (SIF). Guan et al. (2016) provided the first framework to link SIF retrievals to crop yield in the USA from 2007 to 2012 and proposed a new approach for yield estimation. Among abiotic factors, precipitation and temperature have been widely shown to improve crop yield estimation when combined with other satellite-derived variables (Balaghi et al., 2008; Schwalbert et al., 2020; Qader et al., 2023). Additionally, ET, which integrates multiple environmental factors such as precipitation, temperature, and soil moisture, has proven to be an important variable for crop yield estimation (Huang et al., 2015). The theory of de Wit (1958) indicated the linear function between crop yield and ET, which was been further proposed by Stewart and Hagan (1973) and Katerji et al. (1998). Spatially explicit remotely sensed ET data have been related to crop yield by empirical regressions for cereal crops in Ethiopia (Tadesse et al., 2015), wheat yield in Australia (Cai et al., 2019), and maize yield in the United States (Ghazaryan et al., 2020). In addition, the Evaporative Stress Index has shown its capability to explain yield variability in regional- and field-scale studies among the Czech Republic (Anderson et al., 2016a), Brazil (Anderson et al., 2016b), and the United States (Yang et al., 2018). Despite these advancements, no studies have focused on exploring the use of remote sensing-based ET products to estimate crop yield in Sweden.

Process-based crop growth model LPJ-GUESS

Process-based dynamic crop growth models (hereafter referred to as crop models) simulate crop growth and development by modelling the underlying physical and physiological processes (Bouman et al., 1995). LPJ-GUESS is a process-based crop growth model of vegetation dynamics and biogeochemistry, designed for applications ranging from regional to global scales (Smith et al., 2001). The model operates on a daily time step and is driven by a range of climatic variables, including air temperature (°C), precipitation (mm), wind speed (m s^{-1}), relative humidity (%), solar radiation (W m^{-2}), atmospheric CO_2 concentration, and nitrogen deposition. The key processes governing crop growth in LPJ-GUESS encompass plant photosynthesis and respiration, soil decomposition, carbon allocation, crop development, soil hydrology, and human management practices such as fertilization, irrigation, and harvest (Lindeskog et al., 2013; Olin et al., 2015a). Crops in LPJ-GUESS are represented by 11 distinct plant functional types, each characterized by specific temperature requirements for sowing, heat requirements for growth, and carbon allocation patterns (Bondeau et al., 2007; Waha et al., 2012). Carbon allocation to different crop organs is regulated by the accumulated heat units over the growing season, with the potential heat unit sum for each crop type dynamically calculated based on the mean air temperature over the preceding 10 years from the sowing date to the end of the sampling period (Lindeskog et al., 2013). Furthermore, Smith et al. (2014) incorporated nitrogen cycling and limitation into the model, enhancing LPJ-GUESS's capability to simulate biogeochemical feedback, thereby establishing it as one of the most comprehensive crop models available today. Subsequent improvements by Olin et al. (2015a) introduced management options such as irrigation, tillage, and inter-growing season grass cover into the crop module. Except for sowing and irrigation, crops in LPJ-GUESS are assumed to be grown under consistent management practices, nutrient levels, and pest pressures across all grid cells (Bodin et al., 2016). Crop yield outputs from LPJ-GUESS are provided as annual yield data, offering crucial insights into long-term agricultural productivity.

The simulation of a particular area or grid cell in the LPJ-GUESS model typically follows two or three distinct phases. The process begins with the "bare ground" state, where the modelled area is devoid of vegetation. The first phase, known as the "spin-up" phase, involves the gradual accumulation of vegetation, soil, and litter carbon pools until they reach an equilibrium with the prevailing climate conditions. This equilibrium serves as the baseline for the subsequent "historical" phase, during which the model is driven by observational climate data, soil properties, atmospheric CO_2 concentrations, and other environmental variables. In many cases, a third "scenario" phase follows, simulating future climate change projections, which will be discussed in detail in the later chapter.

Integrating satellite remote sensing with crop growth models

Process-based crop growth models are often constrained by inadequate representations of critical internal physical and biological processes within vegetation. This limitation arises from uncertainties in input parameters, such as soil conditions, sowing dates, planting density, and initial field conditions. Parameters utilized in crop models are commonly sourced from existing literature or past experiences and are frequently assumed to be universally applicable across diverse regions (Tubiello et al., 2007; Xiong et al., 2008; De Wit et al., 2010; Lobell et al., 2013). Such generalized parameterizations often fail to account for region-specific environmental conditions, crop varieties, and management practices (Chang et al., 2023), which can result in inaccuracies in simulating crop growth processes and further in simulating the crop yield (Jin et al., 2018). Therefore, the integration of satellite-based data with crop growth models has gained increasing recognition over the past two decades as a promising approach to enhance crop growth simulations and improve crop yield estimation accuracy at the regional levels (Clevers and Leeuwen, 1996; de Wit et al., 2007; Mo et al., 2005; Liang and Qin, 2008; Chen and Tao, 2020).

Currently, three primary methods are employed to integrate remote sensing observations into crop growth models: (1) forcing, (2) assimilation, and (3) calibration (Delécolle et al., 1992; Dorigo et al., 2007). The forcing method utilizes remote sensing data as input to drive crop growth models. Crop models rely on the observed state variables rather than their own predictive mechanisms, which may incorporate inherent errors present in remote sensing data. Assimilation involves continuously updating the crop model simulation under the premise that improving simulation data at a certain time enhances the accuracy of subsequent predictions (Jin et al., 2018). The assimilation method can minimize errors brought into crop growth models during the process. However, it requires the most expensive calculation and information on measurement uncertainty (Jin et al., 2018). In addition, the dates of selected remote sensing images and phenological shifts can also affect the final estimation results (Curnel et al., 2011). In the calibration method, the initial parameters of crop growth models are adjusted to reduce discrepancies between model outputs and satellite-derived variables, which serve as reference data. Compared to the first two methods, model calibration offers greater flexibility and introduces minimized errors from the reference data into the crop model during the calibration process (Jin et al., 2018). In this regard, the calibration method was selected and focused on this PhD project to improve the model performance of crop yield simulation.

Satellite remote sensing datasets have been largely employed to calibrate the crop growth-based parameters across various spatial resolutions, including LAI (Tripathy et al., 2013; Jiang et al., 2014; Yao et al., 2015), NDVI (Fang et al., 2011), the estimated interception efficiency index (Morel et al., 2012), the fraction of absorbed photosynthetically active radiation (Morel et al., 2014), aboveground nitrogen accumulation (Jongschaap, 2006), soil moisture (Eini et al., 2023), and phenological dates (Jongschaap and Schouten, 2005). ET represents the combined water loss from soil and plant surfaces, which directly links to the carbon dioxide assimilation in plants, making it a key variable for monitoring and estimating the agricultural production (Senay et al., 2011). As mentioned in the last chapter, satellite-based ET datasets have been widely used in remote sensing-based empirical models for crop yield estimation. Nevertheless, the use of ET datasets to calibrate process-based crop models for enhancing the accuracy of crop yield simulations remains unexplored.

Driving crop growth models with future climate data for crop yield prediction

Climate change is already impacting crop growth worldwide through various mechanisms, primarily driven by rising average and extreme temperatures, altered precipitation patterns, and elevated atmospheric CO_2 concentrations (Jägermeyr et al., 2021). At the global scale, climate change is expected to pose challenges in increasing yields (Foley et al., 2011). Rising temperatures will exacerbate drought stress, accelerate crop development, and increase yield variability and the risk of yield loss (Lobell et al., 2011). However, at higher latitudes, elevated CO_2 levels and warmer temperatures may boost yields by extending the growing season in temperate and cold regions (Webber et al., 2018; Rezaei et al., 2023). In Scandinavia, elevated atmospheric CO_2 concentrations have been observed to enhance yields of C3 cereals, such as wheat, by effectively fertilizing the crops and increasing their organic matter inputs (Rötter et al., 2011; Lugato et al., 2014; Wiréhn, 2018; Makowski et al., 2020). Lobell et al. (2011) suggested that mid-to-high latitude regions may be well-positioned to adapt agricultural production to climate change, with rising temperatures potentially creating opportunities for increased crop production. Additionally, studies by Peltonen-Sainio et al. (2009) and Olesen et al. (2011) indicated that warmer temperatures could boost crop yields by extending the growing season and reducing the likelihood of frost in the Nordic Region.

Process-based crop growth models forced with future climate data have been extensively utilized to systematically assess agricultural production potential under the projected climatic conditions (Porter et al., 1995; White et al., 2004; Müller et al., 2017; Jägermeyr et al., 2021). Bias-corrected weather data, commonly used as climate input for models, are primarily derived from the Coupled Model Intercomparison Project (CMIP). CMIP5 (Taylor et al., 2012) and CMIP6 (Eyring et al., 2016) have been currently employed for crop yield prediction. CMIP5 included 40 CO_2 concentration-driven General Circulation Models (GCMs) and Earth System Models (ESMs) from 20 research institutions (Kamworapan and Surussavadee, 2019), while CMIP6 expanded to over 100 models contributed by more than 50 modelling centers worldwide. GCM/ESM simulations are available for both historical and future periods. For future projections, each GCM operates under different scenarios representing key natural and anthropogenic drivers influencing the climate system. One of the most widely used scenario frameworks is the Representative Concentration Pathways (RCPs), which include four radiative forcing levels—RCP 2.6, RCP 4.5, RCP 6.0, and RCP 8.5—ranging from low to high radiative forcing and atmospheric CO_2 levels (Blanc et al., 2015), as summarized in Table 1.

Table 1 Different scenarios for four RCPs (Moss et al., 2010).

Name	Radiative forcing	Concentration (p.p.m.)	Model providing RCP*
RCP 2.6	Peak at ~3W m^{-2} before 2100 and then declines	Peak at ~490 CO_2-equiv, before 2100 and then declines	IMAGE
RCP 4.5	~4.5W m^{-2} at stabilization after 2100	~650 CO_2-equiv. (at stabilization after 2100)	GCAM
RCP 6.0	~6W m^{-2} at stabilization after 2100	~850 CO_2-equiv. (at stabilization after 2100)	AIM
RCP 8.5	> 8.5 W m^{-2} in 2100	> 1370 CO_2-equiv. in 2100	MESSAGE

*MESSAGE, Model for Energy Supply Strategy Alternatives and their General Environmental Impact, International Institute for Applied Systems Analysis, Austria; AIM, Asia-Pacific Integrated Model, National Institute for Environmental Studies, Japan; GCAM, Global Change Assessment Model, Pacific Northwest National Laboratory, USA (previously referred to as MiniCAM); and IMAGE, Integrated Model to Assess the Global Environment, Netherlands Environmental Assessment Agency, The Netherlands.

The reliability and applicability for regional crop yield prediction are limited by two key challenges. The first challenge lies in the coarse spatial resolution of the climate forcing data. Most previous studies have relied on climate forcing data derived from GCMs or ESMs, such as EC-EARTH (Hazeleger et al., 2010), GFDL-CM3 (Donner et al., 2011), GISS-E2-R (Rind et al., 2020), etc. These models typically offer coarse spatial resolutions, ranging from 100 to 500 km. Such resolutions encompass diverse land surface types, including croplands, forests, and urban areas, which limits their ability to capture the fine-scale heterogeneity essential for representing agricultural systems. To overcome this limitation, convection-permitting regional climate models (CPRCMs) have been developed, operating at much finer spatial resolutions of 1–5 km. These models enable an improved representation of local climate processes and land surface heterogeneity, reducing uncertainties in capturing key climatic features—particularly precipitation patterns and extreme weather events—by better resolving the climate dynamics associated with heterogeneous surfaces (Kendon et al., 2012; Belušić et al., 2020; Lind et al., 2023). Previous research utilizing CPRCM output data has largely focused on improving the accuracy of precipitation forecasting (Pal et al., 2019), characterizing precipitation distribution (Prein et al., 2020), monitoring extreme weather events (Prein et al., 2015), and assessing snowpack and snow cover distribution (Adinolfi et al., 2020). However, the application of CPRCMs for climate change impact assessments in agroecology remains limited (Garcia-Carreras et al., 2015). To the best of our knowledge, no study to date has employed CPRCMs to evaluate climate change impacts on crop yield in Scandinavia, leaving the assessment of climate risk for Scandinavian farming systems largely uncertain under the intensification of future climatic extremes.

The second challenge concerns the lack of model calibration prior to crop yield prediction. As discussed in the previous chapter, model calibration is essential for tailoring model parameters to reflect local conditions, which is crucial for reducing the uncertainty of yield simulations under changing climate conditions. Angulo et al. (2013) highlighted the importance of region-specific calibration in crop yield prediction at the pan-European level, demonstrating that the calibration strategy significantly influenced the extent of simulated climate change impacts. Despite this, only a limited number of studies have calibrated crop models before assessing the impacts of climate change on crop yields across different countries (Tao et al., 2017; Quansah et al., 2020; Wang et al., 2022). To the best of our knowledge, no previous research has undertaken model calibration prior to evaluating the impact of climate change on crop yields in Sweden, nor has any study employed the LPJ-GUESS model for this purpose.

Aims and thesis structure

Building on the gaps and limitations mentioned in the Introduction section, this thesis aims to improve the accuracy of crop yield predictions in Sweden using satellite remote sensing and the ecosystem LPJ-GUESS model. Four specific objectives are addressed in this study:

1. In **Paper I**, the study aims to evaluate the accuracy of various multi-source gridded ET products and two merged ET datasets using the TC-based merging framework across the Nordic Region. Datasets with the lowest errors are used in **Paper II** and **Paper III** to enhance the accuracy of crop yield estimation in Sweden.
2. In **Paper II**, the study aims to estimate the district-level spring barley yield in southern Sweden using various combinations of monthly satellite-based and climate variables and the RF approach.
3. In **Paper III**, the study aims to calibrate multiple crop-growth-related parameters in LPJ-GUESS to improve the district-level spring barley and winter wheat yield simulation accuracy in southern Sweden.
4. In **Paper IV**, the study aims to assess the potential impacts of future climate change on crop yields in southern Sweden by integrating the calibrated LPJ-GUESS model from **Paper III** with the projected climate data under future scenarios.

The structure of the whole thesis, and the connections between each paper are shown in Fig. 1.

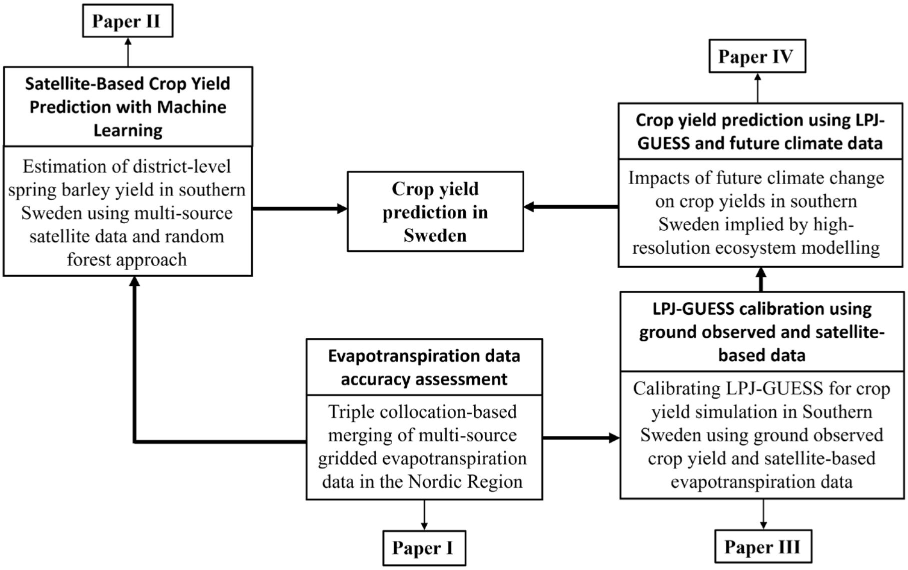

Fig. 1. Illustration of the thesis structure showing the linkages among the four papers included in this study.

Materials and methods

Overview and study area

For the study area, **Paper I** focused on four Nordic countries — Denmark, Sweden, Finland, and Norway — within the Nordic Region, shown in Fig. 2. **Paper II, III, and IV** focused on southern Sweden, including four counties and 17 yield survey districts, shown in Fig. 3 (II) and Fig. 4 (III and IV).

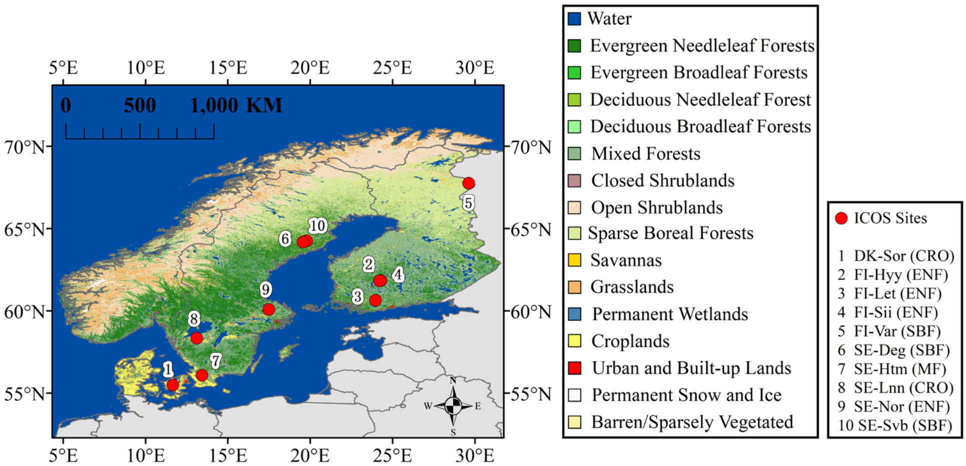

Fig. 2. The land cover classification based on MCD12Q1 of the Nordic Region, along with the location of 10 ICOS sites (Friedl et al., 2010). ENF, MF, CRO, and SBF are short for evergreen needleleaf forests, mixed forests, croplands, and sparse boreal forests, respectively. If there exists a discrepancy between the vegetation types of MCD12Q1 and ICOS, we use the types labelled by the former one.

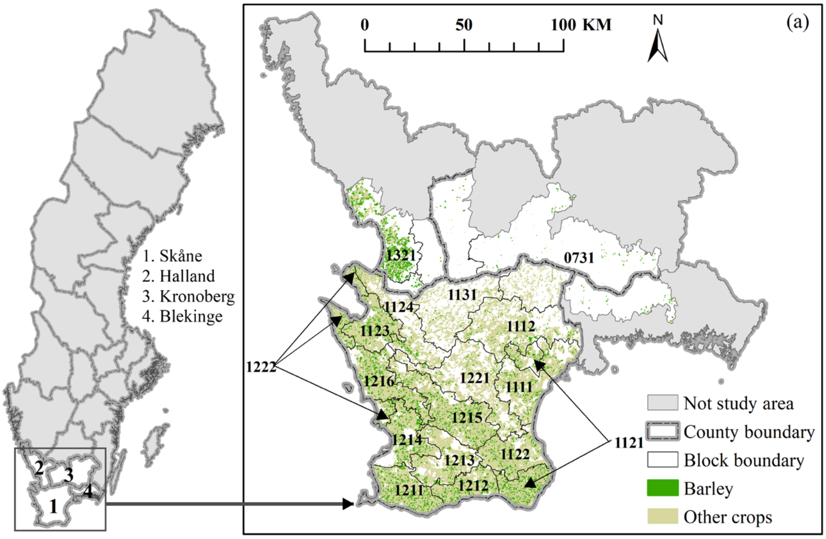

Fig. 3. Distribution map of spring barley fields in southern Sweden in 2022 (SCB, 2023). The distribution of spring barley varies slightly from year to year due to crop rotation. Four-digit numbers indicate district codes.

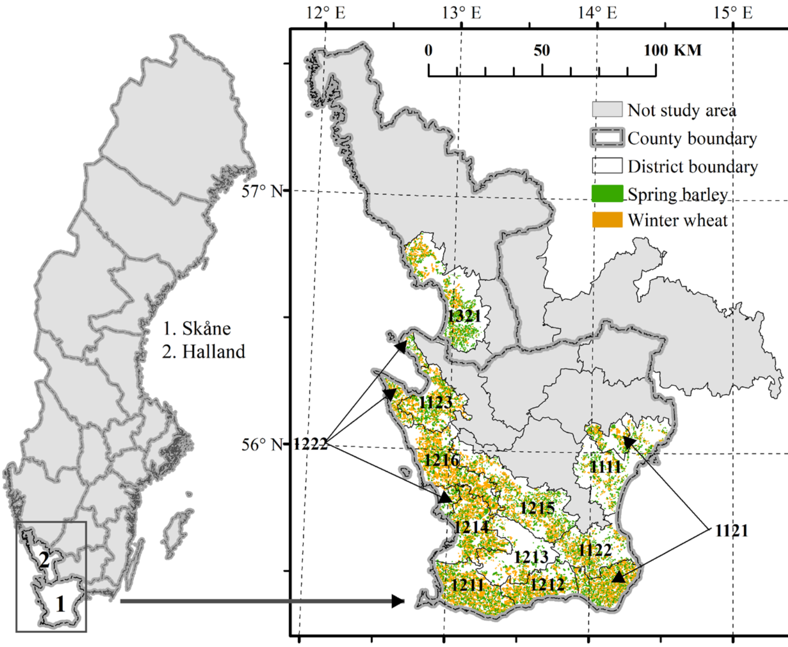

Fig. 4. Distribution map of spring barley and winter wheat fields in southern Sweden in 2022 (SCB, 2023). The distribution of both crops varies slightly from year to year due to crop rotation. Four-digit numbers indicate district codes.

The findings of this thesis were derived using a diverse set of scientific tools and research methods. **Paper I** employed the TC technique to quantify the error structures of global gridded ET products in the Nordic Region. It also evaluated a TC-based merging framework that optimally accounts for the error cross-correlation (ECC) to combine multiple ET products. **Paper II** developed an estimation method using the RF approach, incorporating four satellite-derived products —NDVI, PPI, SIF, and ET — alongside two gridded climate variables: precipitation and air temperature. **Paper III** calibrated six crop growth-based parameters in LPJ-GUESS to enhance the crop yield simulation in southern Sweden using the observed crop yield data and satellite-based ET as reference. **Paper IV** utilized the calibrated LPJ-GUESS from **Paper III** to project district-level spring barley and winter wheat yield, driven by the 3-km high-resolution climate data.

Paper I

TC approach assumes three collocated and independent measurement systems that are all related to the unknown "truth" in the linear additive error model (McColl et al., 2014; Chen, et al., 2017, 2021, Equation 1):

$$ET_i = \alpha_i + \beta_i t + \varepsilon_i \tag{1}$$

where ET_i represents a random ET time-series data (using X, Y and Z as a triplet example, $i \in [X, Y, Z]$); α_i and β_i represent the ordinary least squares intercepts (additive biases) and slopes (multiplicative biases) in the ET dataset *i*; *t* represents the unknown ET reference dataset; and ε_i represents the zero-mean random errors (noises) of the ET dataset i.

Four selected ET products in our study (Table 2) were transformed into zero-mean anomaly time series before applying the TC approach (Chen et al., 2017). Anomalies were calculated against the long-term seasonality (also referred to as climatology), defined as the average value for the same day of the year over their overlapping period (Liu et al., 2012; Peng et al., 2021), as described in Equation 2.

$$ANO_{DOY}^{YR} = ORI_{DOY}^{YR} - \frac{(\sum_{YR=2003}^{2018} ORI_{DOY}^{YR})}{N} \tag{2}$$

where ANO represents the anomalies; YR represents the year from 2003 to 2018; DOY represents the day of the year; ORI represents the original time series of ET estimates; and N represents the number of the years with valid ET estimates.

Table 2 Summary of the four used gridded ET products.

Product	Temporal Resolution	Temporal extent	Spatial resolution	Data unit
FLUXCOM	8-day	2001–2019	0.083°	MJ m^{-2} day^{-1}
GLASS	8-day	2000–2018	0.05°	W m^{-2}
GLEAM v3.5b	daily	2003–2020	0.25°	mm day^{-1}
PML-V2	8-day	2002–2019	0.05°	mm day^{-1}

The difference notation of the TC approach was selected in this study, which is more widely applied in previous research (Gruber et al., 2016). It provided unscaled error variances, presented as absolute error variances, and rescaled error variances for estimating ET merging weights (Draper et al., 2013). The error variances of the unscaled/rescaled ET anomalies were calculated as (Equation 3) (Gruber et al., 2016):

$$\begin{aligned} \sigma_{\varepsilon_X}^2 &= \sigma_{\varepsilon_{X^*}}^2 = \langle (X^* - Y^*)^T (X^* - Z^*) \rangle \\ {\beta_Y^*}^2 \sigma_{\varepsilon_Y}^2 &= \sigma_{\varepsilon_{Y^*}}^2 = \langle (Y^* - X^*)^T (Y^* - Z^*) \rangle, \beta_Y^* = \frac{\sigma_{XZ}}{\sigma_{YZ}} \\ {\beta_Z^*}^2 \sigma_{\varepsilon_Z}^2 &= \sigma_{\varepsilon_{Z^*}}^2 = \langle (Z^* - X^*)^T (Z^* - Y^*) \rangle, \beta_Z^* = \frac{\sigma_{XY}}{\sigma_{YZ}} \end{aligned} \tag{3}$$

where $\sigma_{\varepsilon_X}^2$ represents the error variances of the unscaled data anomaly X (same for other datasets); $\sigma_{\varepsilon_{X^*}}^2$ represents the error variances of the rescaled data anomaly X^* (same for other datasets); σ_{XY} represents the temporal covariance of X and Y (same for other anomaly datasets), and $\langle \cdot \rangle$ represents the temporal average.

The ET merging weights were identified by the error variances of the rescaled ET data anomalies (Dong et al., 2020; Zhou et al., 2021) (using X, Y and Z as a triplet example, Equation 4):

$$\begin{aligned} w_X &= \frac{\sigma_{\varepsilon_{Y^*}}^2 \sigma_{\varepsilon_{Z^*}}^2}{\sigma_{\varepsilon_{X^*}}^2 \sigma_{\varepsilon_{Y^*}}^2 + \sigma_{\varepsilon_{X^*}}^2 \sigma_{\varepsilon_{Z^*}}^2 + \sigma_{\varepsilon_{Y^*}}^2 \sigma_{\varepsilon_{Z^*}}^2} \\ w_Y &= \frac{\sigma_{\varepsilon_{X^*}}^2 \sigma_{\varepsilon_{Z^*}}^2}{\sigma_{\varepsilon_{X^*}}^2 \sigma_{\varepsilon_{Y^*}}^2 + \sigma_{\varepsilon_{X^*}}^2 \sigma_{\varepsilon_{Z^*}}^2 + \sigma_{\varepsilon_{Y^*}}^2 \sigma_{\varepsilon_{Z^*}}^2} \\ w_Z &= \frac{\sigma_{\varepsilon_{X^*}}^2 \sigma_{\varepsilon_{Y^*}}^2}{\sigma_{\varepsilon_{X^*}}^2 \sigma_{\varepsilon_{Y^*}}^2 + \sigma_{\varepsilon_{X^*}}^2 \sigma_{\varepsilon_{Z^*}}^2 + \sigma_{\varepsilon_{Y^*}}^2 \sigma_{\varepsilon_{Z^*}}^2} \end{aligned} \tag{4}$$

The least-square-based optimal merging of the ET anomalies was then calculated as (Equation 5):

$$ET_m = w_X X^* + w_Y Y^* + w_Z Z^* \tag{5}$$

The multi-source merged ET dataset was finally achieved by adding the climatology /seasonal variability to ET_m (Dong et al., 2020).

It is worth mentioning that if there existed multiple (over three) datasets, quadruple collocation (QC) approach should be applied to calculate ECC for each data pair, generating triplets for the TC algorithm. In a triplet, the errors from each dataset should be uncorrelated with each other (Chen et al., 2018). Therefore, the dataset pairs with non-negligible ECC errors, should not appear in the same triplet. If the nonzero ECC only exists between X and Y (the same applies to other data pairs), then the calculation of the ECC value is shown in Equation 6:

$$ECC_{XY} = \frac{\sigma_{\varepsilon_X \varepsilon_Y}}{\sqrt{\sigma^2_{\varepsilon_X} \sigma^2_{\varepsilon_Y}}} \tag{6}$$

Finally, four different statistical comparison metrics including Root Mean Squared Error (RMSE) (Equation 7), Mean Absolute Error (MAE) (Equation 8), unbiased RMSE (ubRMSE) (Equation 9), and the correlation coefficient (R) (Equation 10) were applied for the statistical analysis at each site against the Integrated Carbon Observation System (ICOS) observed data shown in Fig. 2.

$$\text{RMSE} = \sqrt{\frac{\sum_{a=1}^{N} (ET_a - G_a)^2}{N}} \tag{7}$$

$$\text{MAE} = \frac{\sum_{a=1}^{N} |ET_a - G_a|}{N} \tag{8}$$

$$\text{ubRMSE} = \sqrt{\frac{\sum_{a=1}^{N} \left((ET_a - \overline{ET}) - (G_a - \bar{G})\right)^2}{N}} \tag{9}$$

$$\text{R} = \frac{\sum_{a=1}^{N} (ET_a - \overline{ET})(G_a - \bar{G})}{\sqrt{\sum_{a=1}^{N} (ET_a - \overline{ET})^2} \sqrt{\sum_{a=1}^{N} (G_a - \bar{G})^2}} \text{ , } -1 \le \text{R} \le 1 \tag{10}$$

where ET represents four datasets (X, Y, Z and W) and the merged ET datasets, respectively; G represents the ICOS flux data; a represents the ath ET data of the whole ET time-series data; N represents the range of a, which depends on the available years of ICOS flux data (one year contains 46 8-day ET data); and $\overline{ET}$ and $\bar{G}$ represent the mean ET values (within the available years of each site) of four datasets and merged datasets, respectively.

Paper II

Four satellite-derived variables, two climate variables, and the spring barley yield were gathered from various sources, which were shown in Table 3. The satellite variables were grouped into five combinations: (1) NDVI, (2) VI (NDVI + PPI), (3) SIF, (4) VI + SIF, and (5) VI + SIF + ET, with climate data added to each to test the improvements in the prediction accuracy (LeCun et al., 2015; Cai et al., 2019; Cao et al., 2021). Pearson correlation analysis was then applied to remove monthly variables insignificantly related to barley yield (P > 0.01) to avoid impractical inputs and prevent model overfitting. Finally, all satellite and climate variables were input into the RF approach to compare prediction performance across the ten above-mentioned combinations.

Table 3 Summary of the collected datasets for barely yield estimation.

Category	Variables	Temporal Resolution	Spatial resolution	Source	Abbreviations
Crop yield	Barley yield	Annual	District	Jordbruksverket och SCB (www.jordbruksverket.se)	Yield
Satellite imagery	NDVI, PPI	5-day	10 m	High-Resolution Vegetation Phenology and Productivity product suite (https://www.wekeo.eu/)	-
	CSIF	4-day	0.05°	Global spatially contiguous SIF dataset (Zhang et al., 2018)	SIF
	ET	Daily	0.25°	Global Land Evaporation Amsterdam Model (https://www.gleam.eu)	-
Climate	Air temperature, Precipitation	Daily	4 km	Swedish Meteorological and Hydrological Institute (https://www.smhi.se/data/ladda-ner-data/griddade-nederbord-och-temperaturdata-pthbv)	Tmean, Tmax, Tmin, Pmean, Pmax

RF (Breiman, 2001) has been widely implemented in crop yield estimation (Kang et al., 2022). RF has advantages in its ease of training, minimal sensitivity to outliers, high computational efficiency, and resilience against overfitting (Shao et al., 2015). The modelling process consisted of three steps. First, data from all districts (2017–2021) were randomly split into a training set (70%) and a testing set (30%). Second, two key hyperparameters ntree (number of trees) and mtry (number of features for the best split) were tuned using 10-fold cross-validation on the training data (Fushiki, 2011). Third, the optimized model was tested on the testing data to calculate the predicted R^2 and RMSE. This process was repeated 100 times to improve model robustness and minimize the impact of random data splits (Zhou et al., 2022), with the average predicted R^2 and RMSE used to evaluate model performance.

To assess the practical performance of the model, each optimized model from the previous step was used to predict barley yield for 2022. The training data remained unchanged, while the 2022 variables served as the testing data. The average predicted yield (based on 100 runs) for each combination was compared with the observed barley yield in 2022 using the percentage error (i.e., 100 × ((predicted yield–observed yield)/observed yield).

Paper III

For the model calibration process, six yield-related crop parameters (Fig. 5) were selected based on a literature review and expert knowledge of the LPJ-GUESS model (Wu et al., 2018; Xu et al., 2018), with their ranges outlined in Table 4. These parameters include: (1) the minimum C:N ratio (CNmin), indicating the maximum N level in leaves; (2) the C:N ratio range (CNran), a scaling factor determining the maximum C:N ratio; (3) the retranslocation of nitrogen and carbon (Nret and Cret) to grains during senescence; (4) the nitrogen extinction coefficient (kN), describing the vertical decline in leaf nitrogen concentration; and (5) the reduction in nitrogen demand by leaves after anthesis (Ndred). These parameters are essential for simulating light extinction, carbon allocation, and nitrogen and carbon retranslocation, which are critical for yield simulation in LPJ-GUESS (Camargo-Alvarez et al., 2023).

The model was calibrated using observed crop yield and satellite-based ET data from the growing season (April to June), respectively. The amount of crop yield could influence the optimal selection of parameters during the calibration process (Camargo Alvarez et al., 2023). Therefore, the twelve districts in the study area were categorized into low-yield (1111, 1123, 1213, 1215, 1222, 1321) and high-yield groups (1121, 1122, 1211, 1212, 1214, 1216) based on the annual yield production. Two districts with intermediate yields (1123 and 1214) were chosen for calibration. A total of 9072 simulations were run, combining different parameter levels (7×6×3×3×3×8). The best 100 crop yield parameter combinations, of which the simulated crop yield had the lowest RMSE compared with the reference data (observed crop yield data or satellite-based ET data), were selected to run on the remaining ten districts for validation, with performance assessed using RMSE (Equation 11) and the normalized RMSE (nRMSE) (Equation 12):

$$\mathrm{RMSE} = \sqrt{\frac{1}{N}\sum_{i=1}^{N}(\mathrm{S}_i - O_i)^2} \tag{11}$$

$$\mathrm{nRMSE} = \sqrt{\frac{1}{N}\sum_{i=1}^{N}(\mathrm{S}_i - O_i)^2} \times \frac{100}{O} \tag{12}$$

where S_i is the ith simulated value, O_i is the ith observed value, $\bar{O}$ is the mean of the observed values, $\bar{S}$ is the mean of the simulated values, and N is the total number of paired observed-simulated values.

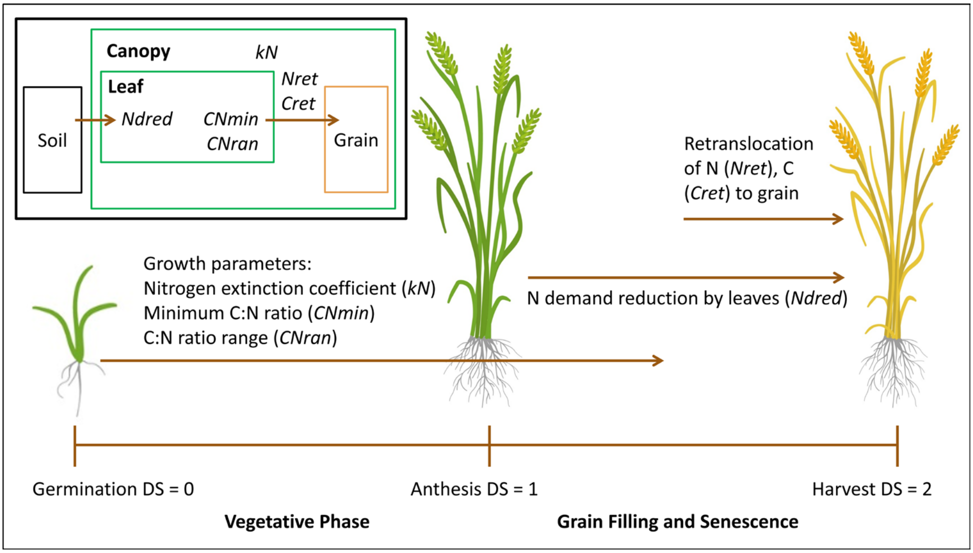

Fig. 5. Diagram of the relationship between calibrated parameters and crop organs during different developmental stages (DS).

Table 4 Parameters for calibration and their ranges, default values for both spring barley (SB) and winter wheat (WW).

Parameter	Abbreviation	Default value	Calibrated ranges	References
Minimum C:N ratio	CNmin	12.5	10, 10.5, 11, 11.5, 12, 12,5, and 13	(Xu et al., 2018)
C:N range	CNran	2.5 (SB), 2 (WW)	2, 2.1, 2.2, 2.3, 2.4, and 2.5	(Camargo-Alvarez et al., 2023)
Retranslocation rate of N	Nret	0.1 day^{-1}	0.05, 0.1, and 0.15 day^{-1}	(Olin et al., 2015b)
Retranslocation rate of C	Cret	0.1 day^{-1}	0.05, 0.1, and 0.15 day^{-1}	(Olin et al., 2015b)
Nitrogen extinction koefficient	kN	0.25 (SB), 0.18 (WW)	0.15, 0.2, and 0.25	(Olin et al., 2015b)
Nitrogen demand reduction factor	Ndred	2.565 (SB), 1.087 (WW)	0, 2, 4, 6, 8, 10, 15, and 20	(Olin et al., 2015b)

Paper IV

In this study, the calibrated LPJ-GUESS model was driven by the daily climate data downscaled from the HCLIM model cycle 38 (HCLIM38) at a 3 km spatial resolution over Fenno-Scandinavia (Lind et al., 2023). Two parent global climate models (GCMs), EC-EARTH (Hazeleger et al., 2012) and GFDL-CM3 (Griffies et al., 2011), were downscaled with HCLIM38 under two emission scenarios: RCP4.5 (for EC-EARTH only) and RCP8.5 (Lind et al., 2023). Climate simulations were conducted for a 20-year historical period (1985–2005) and two future 20-year periods: mid-century (2040–2060) and end-of-century (2080–2100), as shown in Table 5.

Table 5 Description of the 3-km HCLIM38 downscaled climate outputs using two parent GCMs as boundaries under different RCP scenarios and time periods. MC denotes mid-century, and LC denotes end-of-century.

Parent GCM	Climate Scenarios	Period
EC-Earth	-	1985–2005 (Historical)
	RCP4.5	2040–2060 (MC), 2080–2100 (LC)
	RCP8.5	2040–2060 (MC), 2080–2100 (LC)
GFDL-CM3	-	1985–2005 (Historical)
	RCP8.5	2040–2060 (MC), 2080–2100 (LC)

To correct the biases in the HCLIM38 non-bias-corrected climate outputs, a non-parametric empirical quantile mapping (QM) method was applied (Osuch et al., 2017). This adjustment was made for five climate variables: temperature, precipitation, wind speed, relative humidity, and solar radiation. The ERA5-Land reanalysis dataset (https://cds.climate.copernicus.eu/datasets/reanalysis-era5-land?tab=download) served as the reference data for the historical period. The bias correction involved three steps to align the high-resolution 3 km HCLIM38 data with the 0.1° ERA5 data while preserving fine-scale features. First, the HCLIM38 climate data were upscaled from 3 km to 0.1°. Second, the QM method adjusted the full probability distribution of the 0.1° HCLIM38 data using the 0.1° ERA5 data as a reference. Third, the time-series differences between the upscaled HCLIM38 data before and after bias correction were added back to each 3 km HCLIM38 pixel. This ensured the retention of the spatial variability of the high-resolution dataset. For future scenarios, the time-series differences between the 0.1° ERA5 and the 0.1° upscaled HCLIM38 data during the historical period were applied to the corresponding quantiles of the future climate data, enabling consistent redistribution of future projections.

The whole experiment design followed a step-by-step approach to assess crop yield projections. First, observed annual crop yield data at the district level (SCB, 2023) were used to validate the accuracy of simulated crop yield driven by bias-corrected HCLIM38 climate data for the historical period. Second, the calibrated LPJ-GUESS model was driven by bias-corrected HCLIM38 data for two future periods and two emission scenarios, including: (1) EC-EARTH under RCP4.5 (2040–2060); (2) EC-EARTH under RCP8.5 (2040–2060); (3) EC-EARTH under RCP4.5 (2080–2100); (4) EC-EARTH under RCP8.5 (2080–2100); (5) GFDL-CM3 under RCP8.5 (2040–2060); and (6) GFDL-CM3 under RCP8.5 (2080–2100). Third, the annual relative crop yield change (%) from the historical period was calculated to evaluate yield variability under different future periods and RCP scenarios. Finally, the spatial distribution of crop yield for both historical and future periods was visualized to highlight the spatial heterogeneity of spring barley and winter wheat production across different districts. For consistency, the HCLIM38 simulated climate data were referred to as HCLIM38 EC-Earth and HCLIM38 GFDL-CM3 hereafter in the Results and discussion section.

Results and discussion

Error structure of evapotranspiration datasets (Paper I)

Fig. 6 showed the error variances for each ET data anomaly across two triplet groups. FLUXCOM, GLEAM, and PML-V2 consistently had lower error variances than GLASS across the Nordic Region. GLEAM performed especially well in croplands and shrublands, which were more sensitive to drought than taller vegetation. This strong performance was likely due to its use of high-quality satellite-based hydrological data, the TRMM 3B42v7 product (Huffman et al., 2007) and the ESA soil moisture dataset version 2.3 (Liu et al., 2012), both known for their accuracy (Martens et al., 2017).

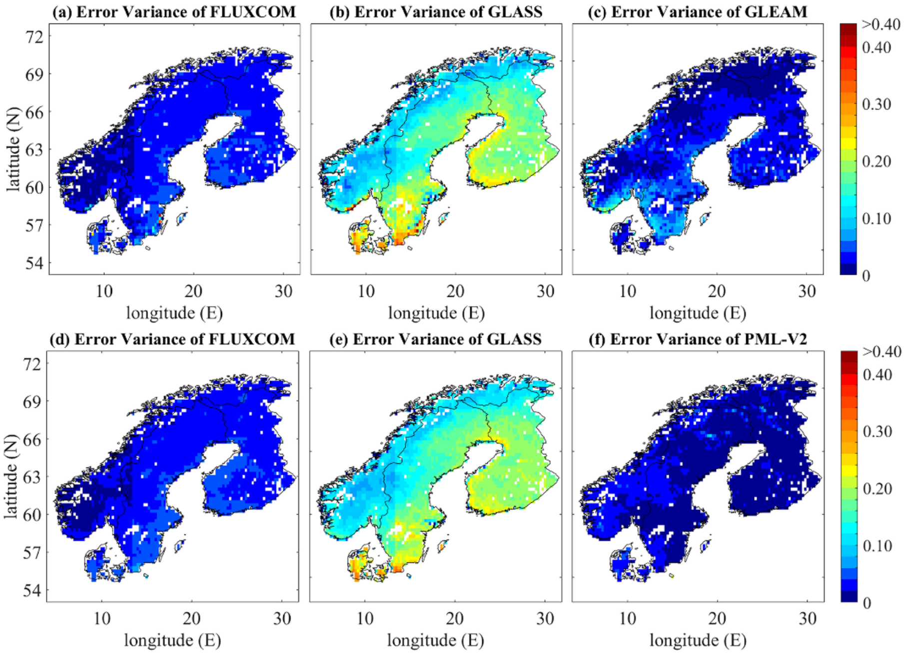

Fig. 6. The TC-based error variances (mm^2 day^{-1}) of each data anomaly in triplet 1: (a) FLUXCOM, (b) GLASS, (c) GLEAM, and triplet 2, (d) FLUXCOM, (e) GLASS, (f) PML-V2.

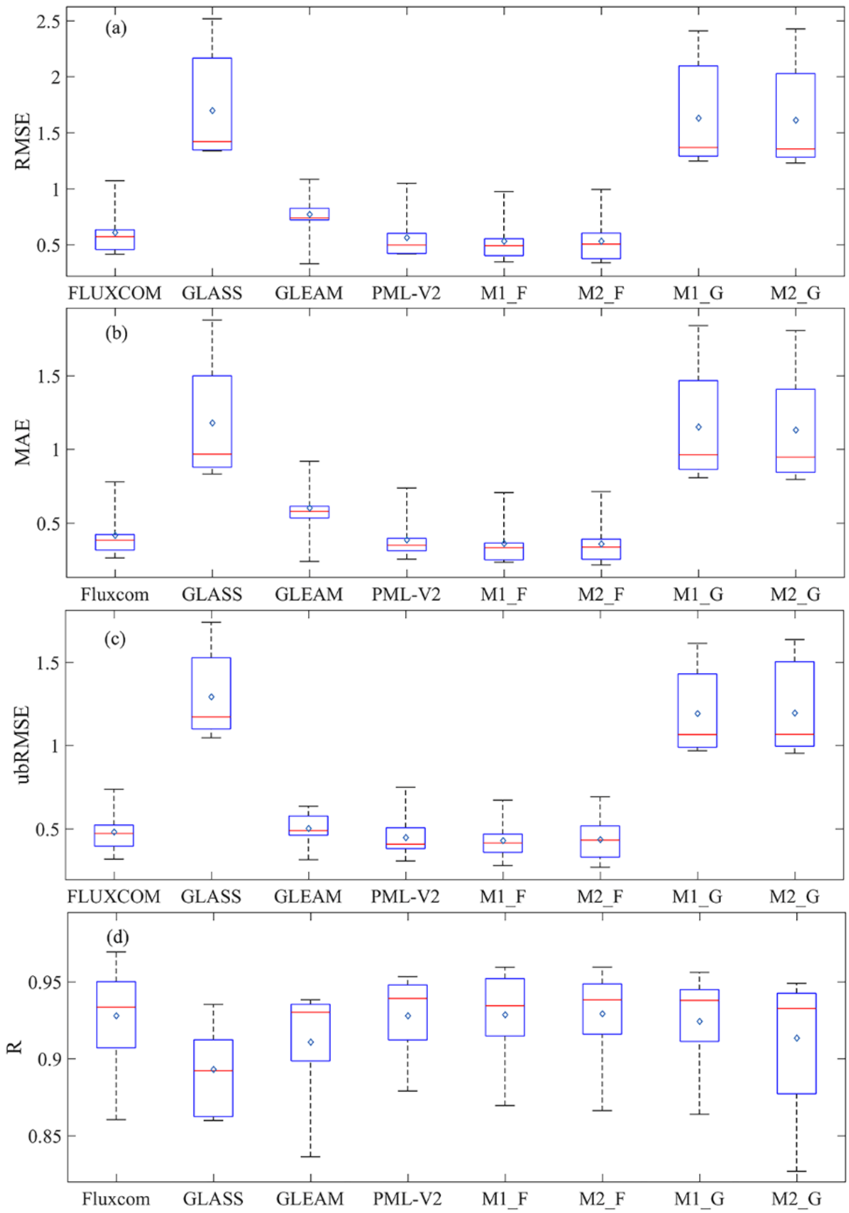

Fig. 7. Statistical comparison between ICOS flux data and six method-derived datasets by means of (a) RMSE (mm day^{-1}), (b) MAE (mm day^{-1}), (c) ubRMSE (mm day^{-1}), and (d) R among 10 ICOS sites. M1_F and M2_F are the merged datasets based on triplet 1 (FLUXCOM, GLASS, and GLEAM) and triplet 2 (FLUXCOM, GLASS, and PML-V2) with FLUXCOM climatology; M1_G and M2_G are the merged datasets based on triplet 1 and triplet 2 with GLASS climatology. Red lines show median values and diamonds show average values.

Fig. 7 compared the statistical metrics of four parent datasets (FLUXCOM, GLASS, GLEAM, and PML-V2) and four merged datasets with different climatology (M1_F, M2_F, M1_G, and M2_G). GLASS had the highest RMSE values (1.34–2.52 mm day^{-1}), while FLUXCOM and GLEAM had lower RMSEs (0.42–1.07 mm day^{-1} and 0.33–1.08 mm day^{-1}, respectively). PML-V2 aligned most closely with the ICOS reference dataset, with RMSE values between 0.42–1.05 mm day^{-1}. The merged datasets M1_F and M2_F had lower average RMSEs (0.56 mm day^{-1} and 0.57 mm day^{-1}) compared to FLUXCOM (0.61 mm day^{-1}), GLASS (1.69 mm day^{-1}), and GLEAM (0.77 mm day^{-1}), and were similar to PML-V2 (0.56 mm day^{-1}). In contrast, M1_G and M2_G only outperformed GLASS, with average RMSEs of 1.62 mm day^{-1} and 1.61 mm day^{-1}. A similar trend was seen in MAE and ubRMSE values. All datasets had R above 0.80 at each site. Given its strong performance, PML-V2 is highly recommended for future hydrological applications, while FLUXCOM and GLEAM also show promise for broader use.

Crop yield prediction using satellite data and random forest approach (Paper II)

The predicted R^2 and RMSE for barley yield estimation using different input combinations were compared (Fig. 8). When using only satellite variables, NDVI and VI performed well, with R^2 values of 0.69 and 0.71 and RMSE of 550 and 533 kg/ha, respectively. SIF alone had lower performance (R^2 = 0.63, RMSE = 595 kg/ha), likely due to its coarse resolution and high noise (Guan et al., 2016). CSIF was used in this study for its higher spatiotemporal resolution compared to other global datasets like GOSAT, GOME-2, and OCO-2. Although TROPOMI SIF offers finer resolution (3.5 km × 5.5 km, daily), it's only available since 2018. Combining SIF and VI significantly improved model performance (R^2 = 0.77, RMSE = 488 kg/ha), showing that SIF provides unique information beyond VIs by capturing short-term climate stresses like heat and water stress and reflecting actual photosynthetic activity (Song et al., 2018; Zhou et al., 2022). Since June variables had a weaker correlation with barley yield, we tested the model using only April and May variables ("VI+SIF_AM" in Fig. 3). This combination also performed well (R^2 = 0.76, RMSE = 499 kg/ha), suggesting that barley yield can be predicted two months before harvest. Adding ET data (VI+SIF+ET) didn't improve performance beyond the VI+SIF combination, likely because using only June's monthly ET data added little value. Despite GLEAM v3.7b ET's coarse spatial resolution (0.25°), its notable correlation with barley yield after resampling suggests ET is a useful indicator for crop yield estimation. Using ET at a finer resolution could further enhance results. Adding climate data to satellite variables didn't significantly improve barley yield predictions (Fig. 8). Previous studies have found overlapping information between VIs and climate data (Cai et al., 2019; Zhou et al., 2022). Shao et al. (2015) also noted that a short climate data record (less than 5–6 years) may not be effective for yield prediction due to yearly climate variations (like drought) and the delayed response of crop growth to climate changes (Seddon et al., 2016).

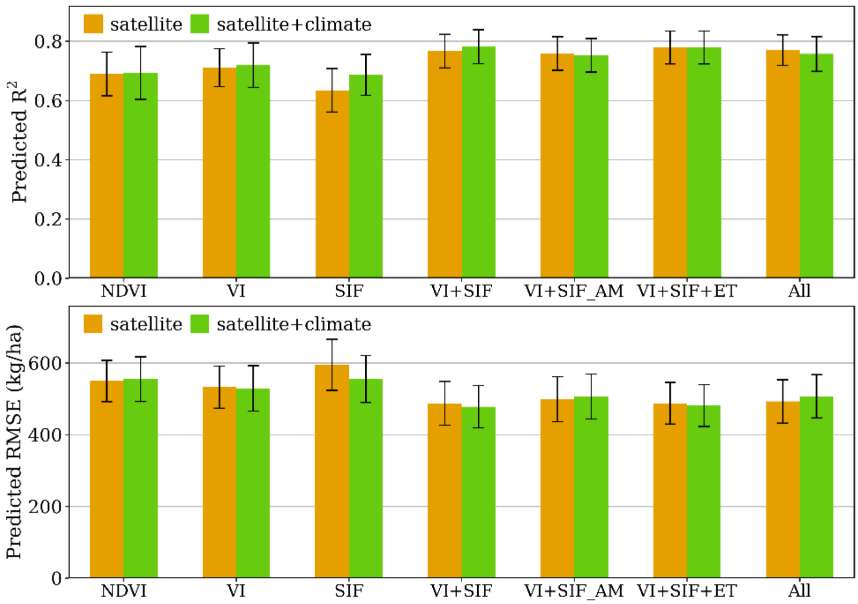

Fig. 8. Testing performance of spring barley yield prediction using both satellite and climate variables in different combinations. The upper and below subfigures represent mean R^2 and RMSE of different combinations, respectively. The error bars are one standard deviation of predicted R^2 and RMSE from 100 ensembles by randomly dividing training and testing dataset. The label "VI+SIF_AM" indicates the model inputs only include the April and May variables in the VI+SIF combination.

To compare model performance with previous studies, we showed the spatial patterns of percentage errors in Fig. 9. Large prediction errors (≥ 20% or ≤ −20%) were only seen in a few districts (1124, 1321, 1211), while most districts had the relative errors between −10% and 10%. These results aligned with the relative errors found in rice yield predictions by Cao et al. (2021) and corn yield predictions by Ma et al. (2021) using the RF model, where most counties had absolute errors below 10%–15%. Districts with the most accurate predictions (errors within −10% to 10%) were mainly in the middle, west coast, and east coast of southern Sweden, where barley is most grown.

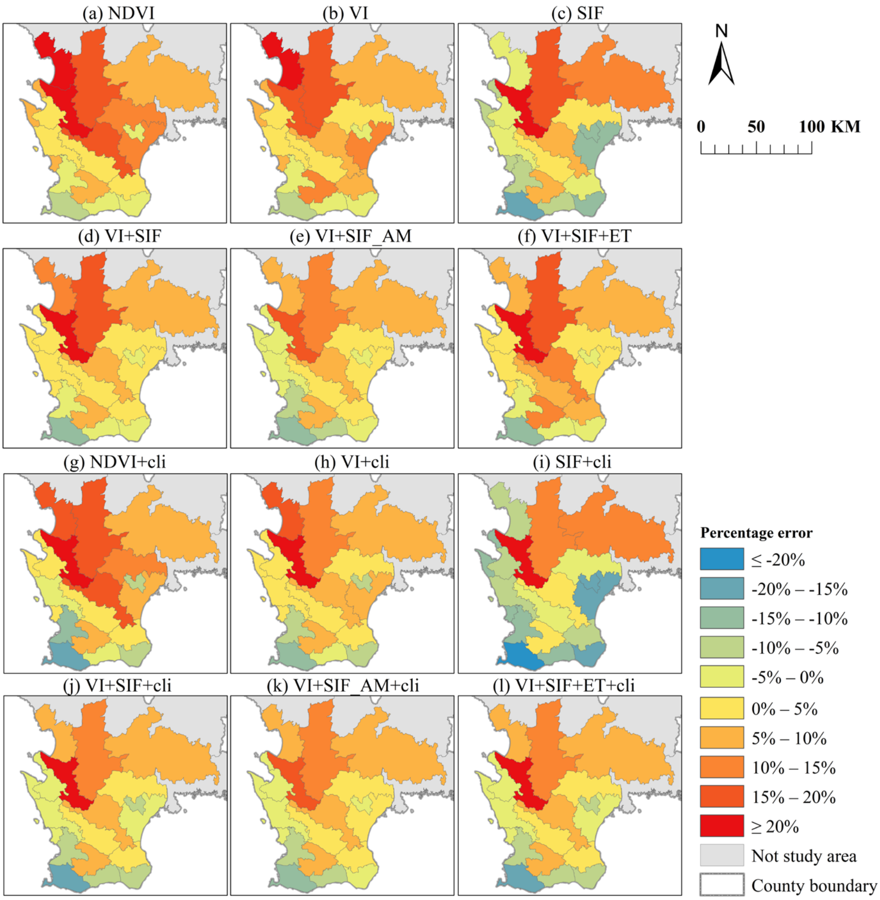

Fig. 9. Spatial distribution of the percentage error of barley yield prediction in 2022 using remote sensing variables (a)–(f), and combining remote sensing and climate (i.e., cli) variables (g)–(l) in different combinations. "AM" in (e) and (k) indicate that the model inputs only include the monthly variables of April and May.

Validation of the calibrated LPJ-GUESS (Paper III)

Fig. 10 showed the validation performance across ten districts using the top 100 parameter combinations (the districts and 100 combinations were detailly described in Paper III). For spring barley, the simulated yield improved significantly in both low- and high-yield districts, with a mean RMSE of 663–788 kg/ha compared to 1784–3431 kg/ha using the default parameters. A similar improvement was seen for winter wheat in high-yield districts, where the mean RMSE dropped from 1095–1746 kg/ha to 815–1150 kg/ha after calibration. In low-yield districts, the accuracy of winter wheat yield increased slightly, with RMSE values of 740–994 kg/ha compared to 745–1044 kg/ha using default parameters. Overall, the mean RMSE across all districts was 710 kg/ha for spring barley and 907 kg/ha for winter wheat, with the mean nRMSE values of 12.8% and 12.2%, respectively. These results highlighted the effectiveness of model calibration using observed crop yield data, especially when compared to the much higher nRMSE values of 50.3% for spring barley and 15.5% for winter wheat using default parameters. As noted by Talebizadeh et al. (2018), using observed crop yield helped directly select the right crop growth parameters suited to site-specific conditions, leading to more accurate yield simulations. The good performance in our study also aligned with previous research using observed crop data for calibration (Liben et al., 2018; Li et al., 2019; Jiang et al., 2021).

The overall validation performance presented in Fig. 11 only demonstrated a slight improvement. The mean RMSE values were 2266 kg/ha (nRMSE = 41.0%) for spring barley and 1056 kg/ha (nRMSE = 14.2%) for winter wheat, both were barely slightly lower than the mean RMSE values without calibration (2786 kg/ha and 1148 kg/ha). Satellite-based evapotranspiration (ET) datasets have been widely applied in crop model assimilation in previous studies. Vazifedoust et al. (2009) and Huang et al. (2015) both assimilated MODIS-derived ET data into the Soil–Water–Atmosphere–Plant (SWAP) model to improve winter wheat yield estimation. The results indicated that the assimilation process had only a slight impact on the accuracy of yield simulations. In the study by Vazifedoust et al. (2009), the yield simulation bias for three individual wheat fields was -30%, 22%, and -10% without calibration, and -31%, 13%, and -5% after calibration. Huang et al. (2015) reported an even greater increase in estimation error, with the mean relative error rising from 6.13% before calibration to 12.86% after calibration. They attributed this poor performance to the heterogeneous agricultural landscape, where the coarse 1-km resolution of the MODIS ET product likely introduced bias by encompassing a mixture of land cover types, including substantial non-wheat areas, when used as reference data for calibration. Although the PML-V2 ET data (0.05°) employed in this study provided higher spatial resolution compared to the simulated ET data (0.1°), it still presented challenges in accurately distinguishing small-scale plots and non-agricultural areas within the study region.

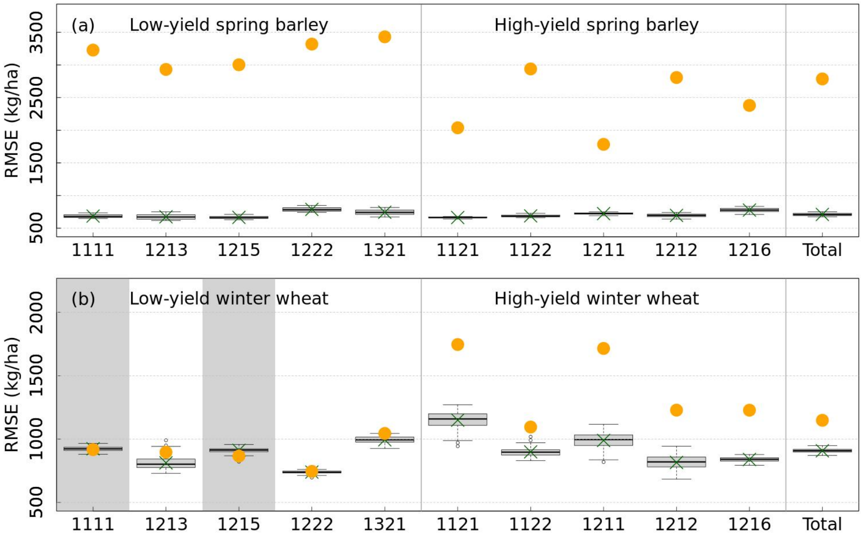

Fig. 10. Comparison of simulated crop yields with and without calibration using RMSE from observed yield data. "Total" shows the average yield across all districts, with grey-shaded areas indicating where calibration didn't reduce RMSE. Yellow dots show RMSE with default parameters.

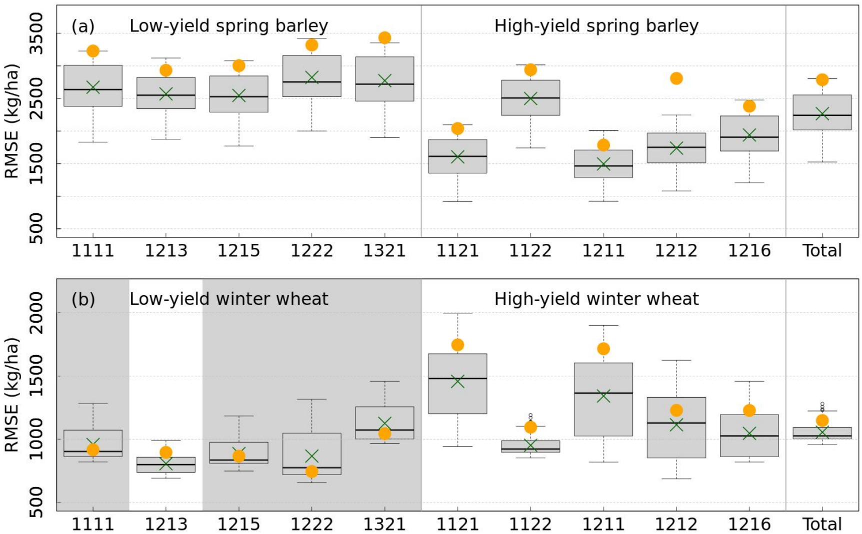

Fig. 11. Comparison of simulated crop yields with and without calibration using RMSE from satellite-based ET data. "Total" shows the average yield across all districts, with grey-shaded areas indicating where calibration didn't reduce RMSE. Yellow dots show RMSE with default parameters.

Crop yield prediction using calibrated LPJ-GUESS and future climate data (Paper IV)

For the relative yield change, both spring barley and winter wheat exhibited similar patterns under future climate scenarios. Therefore, here we focused solely on the yield prediction of spring barley in this analysis, shown in Fig. 12. Compared to the historical period, spring barley yield showed significant increases during the MC and LC periods. In the MC period under the RCP4.5 scenario, spring barley yields increased by 28% in low-yield districts and 25% in high-yield districts for HCLIM38 EC-EARTH. Under the RCP8.5 scenario, the increases were 42% (low-yield) and 40% (high-yield) for HCLIM38 EC-EARTH, and 41% (low-yield) and 37% (high-yield) for HCLIM38 GFDL-CM3. During the LC period, yields increased by 56% (low-yield) and 54% (high-yield) under RCP4.5, and more than doubled (over 100%) under RCP8.5 for both models.

Significant yield losses were observed in the 10th year (i.e., 2089) of the LC period, likely due to insufficient precipitation (i.e., drought) during the growing season (Fig. 13). The average precipitation during the growing season in "normal" years was 269.23 mm, 263.64 mm, and 244.23 mm, respectively, while in 2089, it decreased to 108.32 mm, 56.06 mm, and 66.43 mm. This anticipated yield loss in the projected warm and dry year (i.e., 2089) is consistent with historical observations, as the Nordic Region experienced low wheat and barley yields during the 2018 drought (Mohammadi et al., 2023). De Toro et al. (2015) examined annual yield data at the county level in Sweden for various crops between 1965 and 2014 and found that the lowest yields were typically associated with prolonged dry periods (e.g., < 20 mm of precipitation over 40 days). Additionally, the findings of Beniston et al. (2007) suggest that the projected increase in drought events during the future period (2071–2100) could negatively affect crop production.

The use of high-resolution (3-km) climate data as input for LPJ-GUESS enabled the simulation of the detailed crop yield distributions in each district. Fig. 14–15 show the spatial variability of spring barley and winter wheat yield in the district 1211. Although farmland distribution in southern Sweden varies annually, these fine-resolution yield maps can help identify optimal zones for newly reclaimed agricultural land. Spring barley consistently produced the highest yields in the southwest and the lowest in the northern and eastern parts, across both historical and future periods (Fig. 14). Given the minimal yield differences across different areas, we caution against generalizing this pattern beyond these two districts. Based on these results, for spring barley in district 1211, the southwest appears most suitable for new croplands. For winter wheat, the location of croplands in district 1211 has little impact on overall yield production.

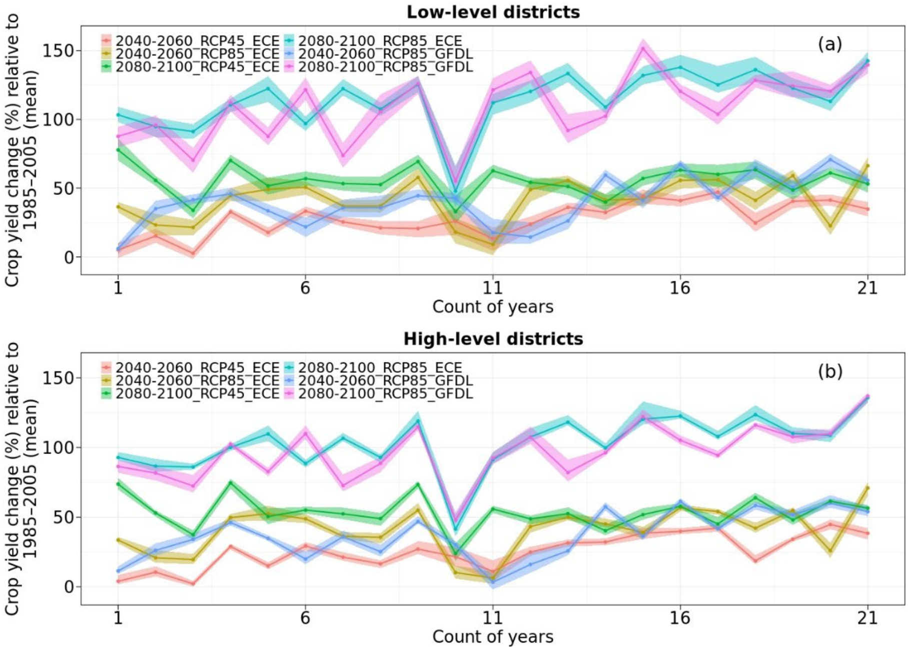

Fig. 12. Mean relative spring barley yield change (%) from the historical period (1985–2005) under different future periods and scenarios. The shadowed areas for each line denote the mean relative changes (%) in spring barley yield simulated for the top 100 parameter combinations selected from the LPJ-GUESS model calibration (paper III).

Fig. 13. Time series of the overall growing season precipitation across all districts over the LC period (2080–2100) under both RCP4.5 and RCP8.5 scenarios.

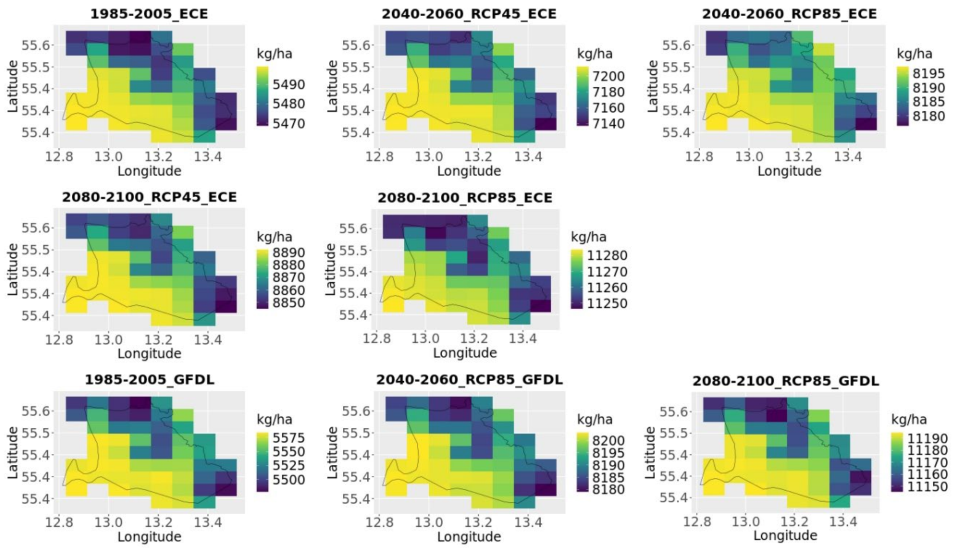

Fig. 14. Average spatial distribution of spring barley yields over historical and future periods in low-yield district 1211.

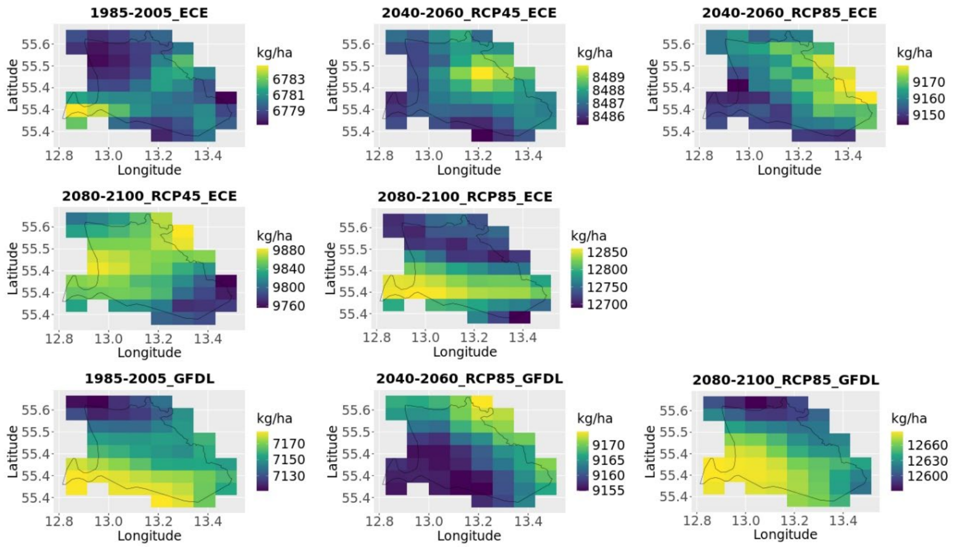

Fig. 15. Average spatial distribution of winter wheat yields over historical and future periods in low-yield district 1211.

Limitations and outlook

Despite the valuable insights gained from this study, several limitations remain and should be addressed in future research, which are summarized from four prospectives corresponding to four papers as follows:

For evaluating the accuracy of multi-source gridded ET data in the Nordic Region (Paper I), discrepancies between flux tower observations and gridded products can lead to spatial representativeness errors. This "mismatch in spatial scale" is a common challenge in the scientific community, requiring collaborative efforts across fields such as measurements, modelling, and satellite remote sensing to find practical solutions in future research. Additionally, we only evaluated four widely used global gridded ET products in the Nordic Region. Future studies should include newly developed global ET products and assess their performance across various spatial and temporal scales. Therefore, further exploration is to study the impact of reference climatology selection on TC-based merging results for different variables and regions.

For crop yield prediction using the satellite-based variables and machine learning technique (Paper II), further enhancements can be achieved by incorporating downscaled datasets with higher spatiotemporal resolution, such as VIs, SIF, climate data, and soil moisture, as inputs to the machine learning model. High-precision remote sensing products are continuously being developed. For instance, the GLEAM4 global ET dataset, which offers daily data from 1980 to 2023 at a 0.1° spatial resolution, has been newly generated (Miralles et al., 2025). We are hopeful that the upcoming high-precision datasets will significantly enhance the accuracy of crop yield estimation and forecasting in the future. Secondly, while RF demonstrated good yield estimation results in this study, exploring other machine learning or deep learning algorithms could potentially yield better performance. Lastly, averaging predictors based on specific phenophases, such as emergence or anthesis periods, rather than using monthly intervals, could reveal more precise relationships between the variables and crop yield. Future research can be extended to a longer time span with more predictors (e.g., sowing dates, soil properties and management practices) for analyzing both spatial and temporal variations in crop yield at the pan-European regional level.

For the LPJ-GUESS model calibration (Paper III), six key parameters were initially calibrated based on prior knowledge. However, this selection may not cover all parameters needed to accurately regulate yield responses. Besides, this study focused on two crop types due to the lack of long-term yield data for other crops like rye and maize. While LPJ-GUESS can simulate up to 11 crop types, more continuous field data is needed to improve yield simulations and achieve more thorough model calibration. Using higher resolution climate and satellite-based ET data could enhance both model performance and calibration accuracy. However, LPJ-GUESS requires significant computation time (~ 10 seconds per simulation per pixel), and finer data would demand more computing power and longer processing times. Thus, optimizing the model's running speed is necessary. Future research should focus on to refining calibration strategies to account for spatial variations in crop growth using high-quality, satellite-based crop growth-based datasets.

For crop yield prediction using the calibrated LPJ-GUESS with future climate data (Paper IV), bias correction was applied to the HCLIM38-simulated 3-km climate data using the 0.1° ERA5-Land reanalysis product as a reference. Any biases in the reanalysis data could carry over to the corrected climate data, potentially affecting crop yield accuracy. Additionally, model validation was done with district-level yield data, which may not fully reflect yield variability at finer spatial scales. However, this is the only long-term crop yield data available in the study area. Lastly, while this study focused on growing-season temperature, precipitation, and crop yields, crop growth is influenced by more complex interactions with other environmental factors. Future research should gather more ground-observed crop yield data at a finer scale and incorporate additional variables to better understand the factors driving yield variability under the impact of climate change.

Conclusions

This thesis conducted a comprehensive investigation into enhancing the accuracy of crop yield prediction in Sweden through two approaches: (1) the integration of satellite-based empirical models with machine learning algorithms and (2) driving the calibrated process-based ecosystem model LPJ-GUESS with the future climate data. Given that both approaches relied on satellite-based ET datasets, a TC-based framework was first employed to select the global gridded ET products with the highest accuracies across the Nordic Region. This study provided valuable insights into the strengths of both approaches, offering a solid foundation for future research and practical applications in Nordic agricultural management. A detailed summary of the key findings from each paper included in this thesis is presented below.

Paper I applied and evaluated the TC technique and TC-based merging framework, offering the first assessment of error structures in four widely used global gridded ET products and two merged ET datasets for the Nordic Region. The study reached three main conclusions. First, the QC-based error cross-correlation calculation effectively identified datasets with the least correlated errors, helping minimize violations of TC assumptions — a crucial step for applying the TC approach. Second, both absolute and relative error variances should be considered when evaluating datasets. Among the four products, PML-V2 showed the best overall performance, with low error variances and a high signal-to-noise ratio. Third, the TC merging technique proved effective for improving ET accuracy in the Nordic Region. Validated against ICOS in situ measurements, the merged ET datasets using FLUXCOM climatology outperformed all parent products in terms of RMSE. However, the choice of climatology can influence the final merged ET results, highlighting the need for further investigation. Beyond supporting dataset selection for **Papers II and III**, our findings have important implications for various applications, such as drought assessment and crop yield estimation.

Paper II focused on estimating district-level spring barley yield in southern Sweden from 2017 to 2022 using satellite data, climate data, and the RF approach. This study found strong positive correlations between barley yield and the monthly average SIF and VIs in April and May, showing that yield can be reliably forecasted two months before harvest. VIs, with their finer spatial resolution, outperformed the coarser-resolution SIF in model predictions. The best results were achieved by combining VIs and SIF, highlighting the unique and valuable information provided by SIF. Adding climate variables did not improve model performance, likely due to their overlapping information with VIs and the short study period. Although adding June's monthly ET contributed little to model performance, its strong correlation with barley yield suggests ET is a promising indicator for yield estimation — one that could perform better with finer spatial resolution. The yield prediction for 2022 showed robust and accurate results, especially in districts with widespread spring barley cultivation. This study proposed a simple and effective framework using freely accessible multi-source data to estimate barley yield, which can also be applicable to other crops and geographic contexts.

Paper III evaluated the performance of LPJ-GUESS with calibration in simulating crop yields at the district level in southern Sweden with a focus on two crop types, spring barley and winter wheat. The model calibration using observed crop yields as reference data significantly improved simulation accuracy for both crop types. Across all studied districts, the mean RMSE was 710 kg/ha for spring barley and 907 kg/ha for winter wheat, with nRMSE values of 12.8% and 12.2%, respectively. This was a major improvement compared to the uncalibrated model, which showed nRMSE values of 50.3% for spring barley and 15.5% for winter wheat. Calibration using the satellite-based ET product PML-V2 during the growing season slightly enhanced simulation accuracy, achieving an nRMSE of 41.0% for spring barley and 14.2% for winter wheat. This highlighted the potential of freely available satellite-based ET products as alternative reference data when observed crop yield data were unavailable. Additionally, the calibrated LPJ-GUESS model effectively assessed drought impacts on crop yields, accurately estimating yield losses for spring barley under drought conditions. Therefore, this calibration approach can effectively improve yield estimation and be used to support agricultural decision-making in Sweden.

Paper IV evaluated the potential impacts of future climate change on crop yields in southern Sweden using the calibrated LPJ-GUESS model from **Paper III**, driven by 3-km high-resolution climate data downscaled through the advanced CPRCM HCLIM38. During the historical period (1985–2005), the simulated yields aligned closely with observed data, demonstrating the model's reliability. Future projections showed significant yield increases, peaking at the end of the century (2080–2100). Under the RCP4.5 scenario, the average simulated yield reached 7753 kg/ha for spring barley and 9043 kg/ha for winter wheat, while in the RCP8.5 scenario, yields rose to 10378 kg/ha and 11411 kg/ha, respectively. In northern Sweden, rising CO_2 levels and higher growing-season temperatures were key drivers of yield improvements. No consistent spatial patterns were observed in low-yield areas, but in high-yield districts like 1211, expanding croplands in the southwest was recommended. These findings highlight the importance of region-specific model calibration when assessing climate change impacts on crop yields and emphasize the need to expand the use of CPRCMs for high-resolution climate simulations across diverse regions in Europe.

References

Adinolfi, M., Raffa, M., Reder, A., Mercogliano, P., 2021. Evaluation and expected changes of summer precipitation at convection permitting scale with COSMO-CLM over Alpine space. Atmosphere, 12(1), 54.

Allen, R.G., Tasumi, M., Trezza, R., 2007. Satellite-based energy balance for mapping evapotranspiration with internalized calibration (METRIC)-Model. Journal of Irrigation and Drainage Engineering, 133(4), 380–394.

Anderson, M.C., Hain, C.R., Jurecka, F., Trnka, M., Hlavinka, P., Dulaney, W., Otkin, J.A., Johnson, D., Gao, F., 2016a. Relationships between the evaporative stress index and winter wheat and spring barley yield anomalies in the Czech Republic. Climate Research, 70, 215–230.

Anderson, M.C., Zolin, C.A., Sentelhas, P.C., Hain, C.R., Semmens, K., Yilmaz, M.T., Gao, F., Otkin, J.A., Tetrault, R., 2016b. The Evaporative Stress Index as an indicator of agricultural drought in Brazil: An assessment based on crop yield impacts. Remote Sensing of Environment, 174, 82–99.

Angulo, C., Rötter, R., Lock, R., Enders, A., Fronzek, S., Ewert, F., 2013. Implication of crop model calibration strategies for assessing regional impacts of climate change in Europe. Agricultural and Forest Meteorology, 170, 32–46.

Azzari, G., Jain, M., Lobell, D.B., 2017. Towards fine resolution global maps of crop yields: Testing multiple methods and satellites in three countries. Remote Sensing of Environment, 202, 129–141.

Baik, J., Park, J., Ryu, D., Choi, M., 2016. Geospatial blending to improve spatial mapping of precipitation with high spatial resolution by merging satellite-based and ground-based data. Hydrological Processes, 30(16), 2789–2803.

Balaghi, R., Tychon, B., Eerens, H., Jlibene, M., 2008. Empirical regression models using NDVI, rainfall and temperature data for the early prediction of wheat grain yields in Morocco. International Journal of Applied Earth Observation and Geoinformation, 10, 438–452.

Belušić, D., de Vries, H., Dobler, A., Landgren, O., Lind, P., Lindstedt, D., Pedersen, R.A., Sánchez-Perrino, J.C., Toivonen, E., van Ulft, B., Wang, F.X., Andrae, U., Batrak, Y., Kjellström, E., Lenderink, G., Nikulin, G., Pietikäinen, J.P., Rodríguez-Camino, E., Samuelsson, P., van Meijgaard, E., Wu, M.C., 2020. HCLIM38: a flexible regional climate model applicable for different climate zones from coarse to convection-permitting scales. Geoscientific Model Development, 13, 1311–1333.

Beniston, M., Stephenson, D.B., Christensen, O.B., Ferro, C.A.T., Frei, C., Goyette, S., Halsnaes, K., Holt, T., Jylhä, K., Koffi, B., Palutikof, J., Schöll, R., Semmler, T., Woth, K., 2007. Future extreme events in European climate: an exploration of regional climate model projections. Climate change, 81, 71–95.

Blanc, E., & Sultan, B., 2015. Emulating maize yields from global gridded crop models using statistical estimates. Agricultural and Forest Meteorology, 214, 134–147.

Bodin, P., Olin, S., Pugh, T.A.M., Arneth, A., 2016. Accounting for interannual variability in agricultural intensification: The potential of crop selection in Sub-Saharan Africa. Agricultural Systems, 148, 159–168.

Bondeau, A., Smith, P.C., Zaehle, S., Schaphoff, S., Lucht, W., Cramer, W., Gerten, D., Lotze-Campen, H., Muller, C., Reichstein, M., Smith, B., 2007. Modelling the role of agriculture for the 20th century global terrestrial carbon balance. Global Change Biology, 13, 679–706.

Bouman, B.A.M., 1995. Crop modeling and remote-sensing for yield prediction. Netherlands Journal of Agricultural Science, 43, 143–161.

Breiman, L., 2001. Random forests. Machine Learning. 45, 5–32.

Byun, K., Liaqat, U.W., Choi, M., 2014. Dual-model approaches for evapotranspiration analyses over homo- and heterogeneous land surface conditions. Agricultural and Forest Meteorology, 197, 169–187.

Cai, Y.P., Guan, K.Y., Lobell, D., Potgieter, A.B., Wang, S.W., Peng, J., Xu, T.F., Asseng, S., Zhang, Y.G., You, L.Z., Peng, B., 2019. Integrating satellite and climate data to predict wheat yield in Australia using machine learning approaches. Agricultural and Forest Meteorology, 274, 144–159.

Camargo-Alvarez, H., Elliott, R.J.R., Olin, S., Wang, X.H., Wang, C.Z., Ray, D.K., Pugh, T.A.M., 2023. Modelling crop yield and harvest index: the role of carbon assimilation and allocation parameters. Modeling Earth Systems and Environment, 9, 2617–2635.

Cao, J., Zhang, Z., Tao, F.L., Zhang, L.L., Luo, Y.C., Zhang, J., Han, J.C., Xie, J., 2021. Integrating multi-source data for rice yield prediction across China using machine learning and dep learning approaches. Agricultural and Forest Meteorology, 297, 108275.

Carletto, C., Jolliffe, D., Banerjee, R., 2015. From tragedy to renaissance: improving agricultural data for better policies. Journal of Development Studies, 51, 133–148.

Chang, Y.B., Latham, J., Licht, M., Wang, L.Z., 2023. A data-driven crop model for maize yield prediction. Communications Biology, 6, 439.

Chen, J.M., & Black, T.A., 1992. Defining leaf-area index for non-flat leaves. Plant Cell and Environment, 15, 421–429.

Chen, F., Crow, W.T., Bindlish, R., Colliander, A., Burgin, M.S., Asanuma, J., Aida, K., 2018. Global-scale evaluation of SMAP, SMOS and ASCAT soil moisture products using triple collocation. Remote Sensing of Environment, 214, 1–13.

Chen, F., Crow, W.T., Ciabatta, L., Filippucci, P., Panegrossi, G., Marra, A.C., Puca, S., Massari, C., 2021. Enhanced large-scale validation of satellite-based land rainfall products. Journal of Hydrometeorology, 22(2), 245–257.

Chen, F., Crow, W.T., Colliander, A., Cosh, M.H., Jackson, T.J., Bindlish, R., Reichle, R.H., Chan, S.K., Bosch, D.D., Starks, P.J., Goodrich, D.C., Seyfried, M.S., 2017. Application of triple collocation in ground-based validation of soil moisture active/passive (SMAP) level 2 data products. IEEE Journal of Selected Topics in Applied Earth Observations and Remote Sensing, 10(2), 489–502.

Chen, Y., & Tao, F.L., 2020. Improving the practicability of remote sensing data-assimilation-based crop yield estimations over a large area using a spatial assimilation algorithm and ensemble assimilation strategies. Agricultural and Forest Meteorology, 291, 108082.

Clevers, J.G.P.W., & vanLeeuwen, H.J.C., 1996. Combined use of optical and microwave remote sensing data for crop growth monitoring. Remote Sensing of Environment, 56, 42–51.

Crow, W.T., Gomez, C.A., Sabater, J.M., Holmes, T., Hain, C.R., Lei, F.N., Dong, J.Z., Alfieri, J.G., Anderson, M.C., 2020. Soil moisture-evapotranspiration overcoupling and L-band brightness temperature assimilation: sources and forecast implications. Journal of Hydrometeorology, 21(10), 2359–2374.

Curnel, Y., de Wit, A.J.W., Duveiller, G., Defourny, P., 2011. Potential performances of remotely sensed LAI assimilation in WOFOST model based on an OSS Experiment. Agricultural and Forest Meteorology, 151, 1843–1855.

Delécolle, R., Maas, S.J., Guerif, M., Baret, F., 1992. Remote-sensing and crop production models - present trends. ISPRS Journal of Photogrammetry and Remote Sensing, 47, 145–161.

De Toro, A., Eckersten, H., Nkurunziza, L., von Rosen, D., 2015. Effects of extreme weather on yield of major arable crops in Sweden. Uppsala.

De Wit, A., Baruth, B., Boogaard, H., van Diepen, K., van Kraalingen, D., Micale, F., Roller, J.T., Supit, I., van den Wijngaart, R., 2010. Using ERA-INTERIM for regional crop yield forecasting in Europe. Climate Research, 44, 41–53.

De Wit, C.T., 1958. Transpiration and crop yield. Versl. Landbouwk. Onderz. 64.6. Inst. of Biol. and Chem. Res. on Field Crops and Herbage, Wageningen, The Netherlands.

De Wit, A.M., & van Diepen, C.A., 2007. Crop model data assimilation with the Ensemble Kalman filter for improving regional crop yield forecasts. Agricultural and Forest Meteorology, 146, 38–56.

Dong, J.Z., Lei, F.N., Wei, L.N., 2020. Triple collocation based multi-source precipitation merging. Frontiers in Water. 2:1.

Dorigo, W.A., Zurita-Milla, R., de Wit, A.J.W., Brazile, J., Singh, R., Schaepman, M.E., 2007. A review on reflective remote sensing and data assimilation techniques for enhanced agroecosystem modeling. International Journal of Applied Earth Observation and Geoinformation, 9, 165–193.

Draper, C., Reichle, R., de Jeu, R., Naeimi, V., Parinussa, R., Wagner, W., 2013. Estimating root mean square errors in remotely sensed soil moisture over continental scale domains. Remote Sensing of Environment, 137, 288–298.

Duan, Z., Duggan, E., Chen, C., Gao, H.K., Dong, J.Z., Liu, J.Z., 2021. Comparison of traditional method and triple collocation analysis for evaluation of multiple gridded precipitation products across Germany. Journal of Hydrometeorology, 22(11), 2983–2999.

Easterling, W.E., Aggarwal, P.K., Batima, P., Brander, K.M., Erda, L., Howden, S.M., Kirilenko, A., Morton, J., Soussana, J.-F., Schmidhuber, J., Tubiello, F.N., 2007. Food, fibre and forest products. In M.L. Change, O.F. Parry, J.P. Canziani, P.J. Palutikof, van der Linden and C.E. Hanson (Eds.), Climate Change 2007: Impacts, Adaptation and Vulnerability. Contribution of Working Group II to the Fourth Assessment Report of the Intergovernmental Panel on Climate. Cambridge University Press, Cambridge, UK, 273–313.

Eini, M.R., Massari, C., Piniewski, M., 2023. Satellite-based soil moisture enhances the reliability of agro-hydrological modeling in large transboundary river basins. Science of the Total Environment, 873, 162396.

Eyring, V., Bony, S., Meehl, G.A., Senior, C.A., Stevens, B., Stouffer, R.J., Taylor, K.E., 2016. Overview of the coupled model intercomparison Project Phase 6 (CMIP6) experimental design and organization. Geoscientific Model Development, 9, 1937–1958.

Fang, H.L., Liang, S.L., Hoogenboom, G., 2011. Integration of MODIS LAI and vegetation index products with the CSM-CERES-Maize model for corn yield estimation. International Journal of Remote Sensing, 32, 1039–1065.

Fisher, J.B., Tu, K.P., Baldocchi, D.D., 2008. Global estimates of the land-atmosphere water flux based on monthly AVHRR and ISLSCP-II data, validated at 16 FLUXNET sites. Remote Sensing of Environment, 112(3), 901–919.

Foley, J.A., Ramankutty, N., Brauman, K.A., Cassidy, E.S., Gerber, J.S., Johnston, M., Mueller, N.D., O'Connell, C., Ray, D.K., West, P.C., Balzer, C., Bennett, E.M., Carpenter, S.R., Hill, J., Monfreda, C., Polasky, S., Rockström, J., Sheehan, J., Siebert, S., Tilman, D., Zaks, D.P.M., 2011. Solutions for a cultivated planet. Nature, 478, 337–342.

Fushiki, T., 2011. Estimation of prediction error by using K-fold cross-validation. Statistics and Computing,. 21, 137–146.

Garcia-Carreras, L., Challinor, A.J., Parkes, B.J., Birch, C.E., Nicklin, K.J., Parker, D.J., 2015. The impact of parameterized convection on the simulation of crop processes. Journal of Applied Meteorology and Climatology, 54, 1283–1296.

Ghazaryan, G., Skakun, S., Koenig, S., Rezaei, E.E., Siebert, S., Dubovyk, O., 2020. Crop yield estimation using multi-source satellite image series and deep learning. IGRASS 2020 - 2020 IEEE International Geoscience and Remote Sensing Symposium, 5163–5166.

Ghilain, N., Arboleda, A., Gellens-Meulenberghs, F., 2011. Evapotranspiration modelling at large scale using near-real time MSG SEVIRI derived data. Hydrology and Earth System Sciences, 15, 771–786.

Griffies, S.M., Winton, M., Donner, L.J., Horowitz, L.W., Downes, S.M., Farneti, R., Gnanadesikan, A., Hurlin, W.J., Lee, H.C., Liang, Z., Palter, J.B., Samuels, B.L., Wittenberg, A.T., Wyman, B.L., Yin, J.J., Zadeh, N., 2011. The GFDL CM3 coupled climate model: Characteristics of the ocean and sea ice simulations. Journal of Climate, 24, 3520–3544.

Godfray, H.C.J., Beddington, J.R., Crute, I.R., Haddad, L., Lawrence, D., Muir, J.F., Pretty, J., Robinson, S., Thomas, S.M., Toulmin, C., 2010. Food security: the challenge of feeding 9 billion people. Science, 327, 812–818.

Gomez-Zavaglia, A., Mejuto, J.C., Simal-Gandara, J., 2020. Mitigation of emerging implications of climate change on food production systems. Food Research International, 137, 109554.

Gruber, A., Su, C.H., Zwieback, S., Crowd, W., Dorigo, W., Wagner, W., 2016b. Recent advances in (soil moisture) triple collocation analysis. International Journal of Applied Earth Observation and Geoinformation, 45, 200–211.

Guan, K.Y., Berry, J.A., Zhang, Y.G., Joiner, J., Guanter, L., Badgley, G., Lobell, D.B., 2016. Improving the monitoring of crop productivity using spaceborne solar-induced fluorescence. Global Change Biology, 22, 716–726.

Hazeleger, W., Wang, X., Severijns, C., Stefanescu, S., Bintanja, R., Sterl, A., Wyser, K., Semmler, T., Yang, S., van den Hurk, B., van Noije, T., van der Linden, E., van der Wiel, K., 2012. EC-Earth V2.2: description and validation of a new seamless earth system prediction model. Climate Dynamics, 39, 2611–2629.

Hersbach, H., Bell, B., Berrisford, P., Hirahara, S., Horanyi, A., Munoz-Sabater, J., Nicolas, J., Peubey, C., Radu, R., Schepers, D., Simmons, A., Soci, C., Abdalla, S., Abellan, X., Balsamo, G., Bechtold, P., Biavati, G., Bidlot, J., Bonavita, M., De Chiara, G., Dahlgren, P., Dee, D., Diamantakis, M., Dragani, R., Flemming, J., Forbes, R., Fuentes, M., Geer, A., Haimberger, L., Healy, S., Hogan, R.J., Holm, E., Janiskova, M., Keeley, S., Laloyaux, P., Lopez, P., Lupu, C., Radnoti, G., de Rosnay, P., Rozum, I., Vamborg, F., Villaume, S., Thepaut, J.N., 2020. The ERA5 global reanalysis. Quarterly Journal of the Royal Meteorological Society, 146(730), 1999–2049.

Huang, J.X., Ma, H.Y., Su, W., Zhang, X.D., Huang, Y.B., Fan, J.L., Wu, W.B., 2015a. Jointly assimilating MODIS LAI and ET products into the SWAP model for winter wheat yield estimation. IEEE Journal of Selected Topics in Applied Earth Observations and Remote Sensing, 8, 4060–4071.

Huete, A., Didan, K., Miura, T., Rodriguez, E.P., Gao, X., Ferreira, L.G., 2002. Overview of the radiometric and biophysical performance of the MODIS vegetation indices. Remote Sensing of Environment, 83, 195–213.

Huffman, G.J., Adler, R.F., Bolvin, D.T., Gu, G.J., Nelkin, E.J., Bowman, K.P., Hong, Y., Stocker, E.F., Wolff, D.B., 2007. The TRMM multisatellite precipitation analysis (TMPA): Quasi-global, multiyear, combined-sensor precipitation estimates at fine scales. Journal of Hydrometeorology, 8(1), 38–55.

Huete, A.R., 1988. A soil-adjusted vegetation index (SAVI). Remote Sensing of Environment, 25, 295–309.

Hunter, M.C., Smith, R.G., Schipanski, M.E., Atwood, L.W., Mortensen, D.A., 2017. Agriculture in 2050: Recalibrating targets for sustainable intensification. Bioscience, 67, 385–390.

Jägermeyr, J., Müller, C., Ruane, A.C., Elliott, J., Balkovic, J., Castillo, O., Faye, B., Foster, I., Folberth, C., Franke, J.A., Fuchs, K., Guarin, J.R., Heinke, J., Hoogenboom, G., Iizumi, T., Jain, A.K., Kelly, D., Khabarov, N., Lange, S., Lin, T.S., Liu, W.F., Mialyk, O., Minoli, S., Moyer, E.J., Okada, M., Phillips, M., Porter, C., Rabin, S.S., Scheer, C., Schneider, J.M., Schyns, J.F., Skalsky, R., Smerald, A., Stella, T., Stephens, H., Webber, H., Zabel, F., Rosenzweig, C., 2021. Climate impacts on global agriculture emerge earlier in new generation of climate and crop models. Nature Food, 2, 873–885.

James, M.E., & Kalluri, S.N.V., 1994. The Pathfinder AVHRR land data set: An improved coarse resolution data set for terrestrial monitoring. International Journal of Remote Sensing, 15, 3347–3363.

Jia, Z.Z., Liu, S.M., Xu, Z.W., Chen, Y.J., Zhu, M.J., 2012. Validation of remotely sensed evapotranspiration over the Hai River Basin, China. Journal of Geophysical Research-Atmospheres, 117(D13), D13113.

Jiang, R., Yang, J.Y., Drury, C.F., He, W.T., Smith, W.N., Grant, B.B., He, P., Zhou, W., 2021. Assessing the impacts of diversified crop rotation systems on yields and nitrous oxide emissions in Canada using the DNDC model. Science of the Total Environment, 759, 143433.

Jiang, Z.W., Chen, Z.X., Chen, J., Liu, J., Ren, J.Q., Li, Z.N., Sun, L., Li, H., 2014. Application of Crop Model Data Assimilation with a particle filter for estimating regional winter wheat yields. IEEE Journal of Selected Topics in Applied Earth Observations and Remote Sensing, 7, 4422–4431.

Jin, H.X., & Eklundh, L., 2014. A physically based vegetation index for improved monitoring of plant phenology. Remote Sensing of Environment, 152, 512–525.

Jin, X.L., Kumar, L., Li, Z.H., Feng, H.K., Xu, X.G., Yang, G.J., Wang, J.H., 2018. A review of data assimilation of remote sensing and crop models. European Journal of Agronomy, 92, 141–152.

Johnson, D.M., 2014. An assessment of pre- and within-season remotely sensed variables for forecasting corn and soybean yields in the United States. Remote Sensing of Environment, 141, 116–128.

Jongschaap, R.E.E., 2006. Run-time calibration of simulation models by integrating remote sensing estimates of leaf area index and canopy nitrogen. European Journal of Agronomy, 24, 316–324

Jongschaap, R.E.E., & Schouten, L.S.M., 2005. Predicting wheat production at regional scale by integration of remote sensing data with a simulation model. Agronomy for Sustainable Development, 25, 481–489.

Jung, M., Koirala, S., Weber, U., Ichii, K., Gans, F., Camps-Valls, G., Papale, D., Schwalm, C., Tramontana, G., Reichstein, M., 2019. The FLUXCOM ensemble of global land-atmosphere energy fluxes. Scientific Data, 6, 74.

Kamworapan, S., & Surussavadee, C., 2019. Evaluation of CMIP5 global climate models for simulating climatological temperature and precipitation for Southeast Asia. Advances in Meteorology, 2019, 1067365.

Katerji, N., van Hoorn, J.W., Hamdy, A., Mastrorilli, M., Karam, F., 1998. Salinity and drought, a comparison of their effects on the relationship between yield and evapotranspiration. Agricultural Water Management, 36, 45–54.

Kendon, E.J., Roberts, N.M., Senior, C.A., Roberts, M.J., 2012. Realism of rainfall in a very high-resolution regional climate model. Journal of climate, 25, 5791–5806.

Khan, M.S., Liaqat, U.W., Baik, J., Choi, M., 2018. Stand-alone uncertainty characterization of GLEAM, GLDAS and MOD16 evapotranspiration products using an extended triple collocation approach. Agricultural and Forest Meteorology, 252, 256–268.

Kang, X.Y., Huang, C.P., Zhang, L.F., Zhang, Z., Lv, X., 2022. Downscaling solar-induced chlorophyll fluorescence for field-scale cotton yield estimation by a two-step convolutional neural network. Computers and Electronics in Agriculture, 201, 107260.

LeCun, Y., Bengio, Y., Hinton, G., 2015. Deep learning. Nature. 521, 436–444.

Li, H.M., Stopa, J.E., Mouche, A., Zhang, B., He, Y.J., Chapron, B., 2021. Assessment of ocean wave spectrum using global Envisat/ASAR data and hindcast simulation. Remote Sensing of Environment, 264, 112614.

Li, P., Ren, L., 2019. Evaluating the effects of limited irrigation on crop water productivity and reducing deep groundwater exploitation in the North China Plain using an agro-hydrological model: I. Parameter sensitivity analysis, calibration and model validation. Journal of Hydrology, 574, 497–516.

Liang, S., & Qin, J., 2008. Data assimilation methods for land surface variable estimation. In Advances in Land Remote Sensing: System, Modeling, Inversion and Application, S. Liang (Ed.), New York: Springer, 319–339.

Liben, F.M., Wortmann, C.S., Yang, H., Lindquist, J.L., Tadesse, T., Wegary, D., 2018. Crop model and weather data generation evaluation for conservation agriculture in Ethiopia. Field Crops Research, 228, 122–134.

Lind, P., Belusic, D., Médus, E., Dobler, A., Pedersen, R.A., Wang, F.X., Matte, D., Kjellström, E., Landgren, O., Lindstedt, D., Christensen, O.B., Christensen, J.H., 2023. Climate change information over Fenno-Scandinavia produced with a convection-permitting climate model. Climate Dynamics, 61, 519–541.

Lindeskog, M., Arneth, A., Bondeau, A., Waha, K., Seaquist, J., Olin, S., Smith, B., 2013. Implications of accounting for land use in simulations of ecosystem carbon cycling in Africa. Earth System Dynamics, 4, 385–407.

Liu, Y.Y., Dorigo, W.A., Parinussa, R.M., de Jeu, R.A.M., Wagner, W., McCabe, M.F., Evans, J.P., van Dijk, A.I.J.M., 2012. Trend-preserving blending of passive and active microwave soil moisture retrievals. Remote Sensing of Environment, 123, 280–297.

Lobell, D.B., 2013. The use of satellite data for crop yield gap analysis. Field Crops Research, 143, 56–64.

Lobell, D.B., Hammer, G.L., McLean, G., Messina, C., Roberts, M.J., Schlenker, W., 2013. The critical role of extreme heat for maize production in the United States. Nature Climate Change, 3, 497–501.

Lobell, D.B., Schlenker, W., Costa-Roberts, J., 2011. Climate trends and global crop production since 1980. Science, 333, 616–620.

Lugato, E., Panagos, P., Bampa, F., Jones, A., Montanarella, L., 2014. A new baseline of organic carbon stock in European agricultural soils using a modelling approach. Global Change Biology. 20, 313–326

Ma, Y.C., Zhang, Z., Kang, Y.H., Özdogan, M., 2021. Corn yield prediction and uncertainty analysis based on remotely sensed variables using a Bayesian neural network approach. Remote Sensing of Environment, 259, 112408.

Majozi, N.P., Mannaerts, C.M., Ramoelo, A., Mathieu, R., Mudau, A.E., Verhoef, W., 2017. An intercomparison of satellite-based daily evapotranspiration estimates under different eco-climatic regions in South Africa. Remote Sensing, 9(4), 307.

Makowski, D., Marajo-Petitzon, E., Durand, J.L., Ben-Ari, T., 2020. Quantitative synthesis of temperature, CO_2, rainfall, and adaptation effects on global crop yields. European Journal of Agronomy, 115, 126041.

Mariotto, I., Thenkabail, P.S., Huete, A., Slonecker, E.T., Platonov, A., 2013. Hyperspectral versus multispectral crop-productivity modeling and type discrimination for the HyspIRI mission. Remote Sensing of Environment, 139, 291–305.

Marshall, M., Belgiu, M., Boschetti, M., Pepe, M., Stein, A., Nelson, A., 2022. Field-level crop yield estimation with PRISMA and Sentinel-2. ISPRS Journal of Photogrammetry and Remote Sensing, 187, 191–210.

Martens, B., Miralles, D.G., Lievens, H., van der Schalie, R., de Jeu, R.A.M., Fernandez-Prieto, D., Beck, H.E., Dorigo, W.A., Verhoest, N.E.C., 2017. GLEAM v3: satellite-based land evaporation and root-zone soil moisture. Geoscientific Model Development, 10(5), 1903–1925.

Mateo-Sanchis, A., Piles, M., Munoz-Mari, J., Adsuara, J.E., Perez-Suay, A., Camps-Valls, G., 2019. Synergistic integration of optical and microwave satellite data for crop yield estimation. Remote Sensing of Environment, 234, 111460.

McColl, K.A., Vogelzang, J., Konings, A.G., Entekhabi, D., Piles, M., Stoffelen, A., 2014. Extended triple collocation: Estimating errors and correlation coefficients with respect to an unknown target. Geophysical Research Letters, 41, 6229–6236.

Miralles, D.G., Bonte, O., Koppa, A., Baez-Villanueva, O.M., Tronquo, E., Zhong, F., Beck, H.E., Hulsman, P., Dorigo, W., Verhoest, N.E.C., Haghdoost, S., 2025. GLEAM4: global land evaporation and soil moisture dataset at 0.1° resolution from 1980 to near present. Scientific Data, 12, 416.

Miralles, D.G., Holmes, T.R.H., De Jeu, R.A.M., Gash, J.H., Meesters, A.G.C.A., Dolman, A.J., 2011. Global land-surface evaporation estimated from satellite-based observations. Hydrology and Earth System Sciences, 15(2), 453–469.

Mo, X.G., Liu, S.X., Lin, Z.H., Xu, Y.Q., Xiang, Y., McVicar, T.R., 2005. Prediction of crop yield, water consumption and water use efficiency with a SVAT-crop growth model using remotely sensed data on the North China Plain. Ecological Modelling, 183, 301–322.

Mohammadi, S., Rydgren, K., Bakkestuen, V., Gillespie, M.A.K., 2023. Impacts of recent climate change on crop yield can depend on local conditions in climatically diverse regions of Norway. Scientific Reports, 13, 3633.

Morel, J., Begue, A., Todoroff, P., Martine, J.F., Lebourgeois, V., Petit, M., 2014. Coupling a sugarcane crop model with the remotely sensed time series of fIPAR to optimise the yield estimation. European Journal of Agronomy, 61, 60–68.

Morel, J., Martine, J.F., Begue, A., Todoroff, P., Petit, M., 2012. A comparison of two coupling methods for improving a sugarcane model yield estimation with a NDVI-derived variable. Remote Sensing for Agriculture, Ecosystems, and Hydrology Xiv, 85310E.

Moss, R.H., Edmonds, J.A., Hibbard, K.A., Manning, M.R., Rose, S.K., van Vuuren, D.P., Carter, T.R., Emori, S., Kainuma, M., Kram, T., Meehl, G.A., Mitchell, J.F.B., Nakicenovic, N., Riahi, K., Smith, S.J., Stouffer, R.J., Thomson, A.M., Weyant, J.P., Wilbanks, T.J., 2010. The next generation of scenarios for climate change research and assessment. Nature, 463, 747–756.

Moulin, S., Bondeau, A., Delecolle, R., 1998. Combining agricultural crop models and satellite observations: from field to regional scales. International Journal of Remote Sensing, 19, 1021–1036.

Müller, C., Franke, J., Jagermeyr, J., Ruane, A.C., Elliott, J., Moyer, E., Heinke, J., Falloon, P.D., Folberth, C., Francois, L., Hank, T., Izaurralde, R.C., Jacquemin, I., Liu, W.F., Olin, S., Pugh, T.A.M., Williams, K., Zabel, F., 2021. Exploring uncertainties in global crop yield projections in a large ensemble of crop models and CMIP5 and CMIP6 climate scenarios. Environmental Research Letters, 16, 034040.

Mu, Q., Heinsch, F.A., Zhao, M., Running, S.W., 2007. Development of a global evapotranspiration algorithm based on MODIS and global meteorology data. Remote Sensing of Environment, 111(4), 519–536.

Murthy, C.S., Thiruvengadachari, S., Raji, P.V., Jonna, S., 1996. Improved ground sampling and crop yield estimation using satellite data. International Journal of Remote Sensing, 17, 945–956.

Olesen, J.E., Trnka, M., Kersebaum, K.C., Skjelvåg, A.O., Seguin, B., Peltonen-Sainio, P., Rossi, F., Kozyra, J., Micale, F., 2011. Impacts and adaptation of European crop production systems to climate change. European Journal of Agronomy, 34, 96–112.

Olin, S., Lindeskog, M., Pugh, T.A.M., Schurgers, G., Warlind, D., Mishurov, M., Zaehle, S., Stocker, B.D., Smith, B., Arneth, A., 2015a. Soil carbon management in large-scale Earth system modelling: implications for crop yields and nitrogen leaching. Earth System Dynamics, 6, 745–768.

Olin, S., Schurgers, G., Lindeskog, M., Warlind, D., Smith, B., Bodin, P., Holmer, J., Arneth, A., 2015b. Modelling the response of yields and tissue C : N to changes in atmospheric CO_2 and N management in the main wheat regions of western Europe. Biogeosciences, 12, 2489–2515.

Osborne, T.M., Lawrence, D.M., Challinor, A.J., Slingo, J.M., Wheeler, T.R., 2007. Development and assessment of a coupled crop-climate model. Global Change Biology, 13, 169–183.

Osuch, M., Lawrence, D., Meresa, H.K., Napiorkowski, J.J., Romanowicz, R.J., 2017. Projected changes in flood indices in selected catchments in Poland in the 21st century. Stochastic Environmental Research and Risk Assessment, 31, 2435–2457.

Pal, S., Chang, H.I., Castro, C.L., Dominguez, F., 2019. Credibility of convection-permitting modeling to improve seasonal precipitation forecasting in the southwestern United States. Frontiers in Earth Science, 7, 11.

Peltonen-Sainio, P., Jauhiainen, L., Hakala, K., Ojanen, H., 2009. Climate change and prolongation of growing season: changes in regional potential for field crop production in Finland. Agricultural and Food Science, 18 (3–4), 171–190.

Peng, J., Tanguy, M., Robinson, E.L., Pinnington, E., Evans, J., Ellis, R., Cooper, E., Hannaford, J., Blyth, E., Dadson, S., 2021. Estimation and evaluation of high-resolution soil moisture from merged model and Earth observation data in the Great Britain. Remote Sensing of Environment, 264, 112610.

Porter, J.R., Leigh, R.A., Semenov, M.A., Miglietta, F., 1995. Modelling the effects of climatic change and genetic modification on nitrogen use by wheat. European Journal of Agronomy, 4, 419–429.

Prein, A.F., Langhans, W., Fosser, G., Ferrone, A., Ban, N., Goergen, K., Keller, M., Tölle, M., Gutjahr, O., Feser, F., Brisson, E., Kollet, S., Schmidli, J., van Lipzig, N.P.M., Leung, R., 2015. A review on regional convection-permitting climate modeling: Demonstrations, prospects, and challenges. Reviews of Geophysics, 53, 323–361.

Prein, A.F., Liu, C.H., Ikeda, K., Bullock, R., Rasmussen, R.M., Holland, G.J., Clark, M., 2020. Simulating north American mesoscale convective systems with a convection-permitting climate model. Climate Dynamics, 55, 95–110.

Qader, S.H., Utazi, C.E., Priyatikanto, R., Najmaddin, P., Hama-Ali, E.O., Khwarahm, N.R., Tatem, A.J., Dash, J., 2023. Exploring the use of Sentinel-2 datasets and environmental variables to model wheat crop yield in smallholder arid and semi-arid farming systems. Science of the Total Environment, 869, 161716.

Quansah, J. E., Welikhe, P., El Afandi, G., Fall, S., Mortley, D., Ankumah, R., 2020. CROPGRO-soybean model calibration and assessment of soybean yield responses to climate change. American Journal of Climate Change. 9, 297–316.

Rezaei, E.E., Webber, H., Asseng, S., Boote, K., Durand, J.L., Ewert, F., Martre, P., Maccarthy, D.S., 2023. Climate change impacts on crop yields. Nature Reviews Earth & Environment, 4, 831–846.

Richardson, A.J., & Wiegand, C.L., 1977. Distinguishing vegetation from soil background information. Photogrammetric Engineering and Remote Sensing, 43, 1541–1552.

Rind, D., Orbe, C., Jonas, J., Nazarenko, L., Zhou, T., Kelley, M., Lacis, A., Shindell, D., Faluvegi, G., Romanou, A., Russell, G., Tausnev, N., Bauer, M., Schmidt, G., 2020. GISS model E2.2: A climate model optimized for the middle atmosphere-model structure, climatology, variability, and climate sensitivity. Journal of Geophysical Research: Atmospheres, 125(10), e2019JD032204.

Rodell, M., Houser, P.R., Jambor, U., Gottschalck, J., Mitchell, K., Meng, C.J., Arsenault, K., Cosgrove, B., Radakovich, J., Bosilovich, M., Entin, J.K., Walker, J.P., Lohmann, D., Toll, D., 2004. The global land data assimilation system. Bulletin of the American Meteorological Society, 85(3), 381–394.

Rötter, R.P., Palosuo, T., Pirttioja, N.K., Dubrovsky, M., Salo, T., Fronzek, S., Aikasalo, R., Trnka, M., Ristolainen, A., Carter, T.R., 2011. What would happen to barley production in Finland if global warming exceeded 4°C? A model-based assessment. European Journal of Agronomy, 35, 205–214.

SCB, 2023. Skördar efter län/riket och gröda. År 1965–2023.

Samuel, A., Girma, A., Zenebe, A., Ghebreyohannes, T., 2018. Spatio-temporal variability of evapotranspiration and crop water requirement from space. Journal of Hydrology, 567, 732–742.

Seddon, A.W.R., Macias-Fauria, M., Long, P.R., Benz, D., Willis, K.J., 2016. Sensitivity of global terrestrial ecosystems to climate variability. Nature, 531, 229–232.

Senay, G.B., Budde, M.E., Verdin, J.P., 2011. Enhancing the Simplified Surface Energy Balance (SSEB) approach for estimating landscape ET: Validation with the METRIC model. Agricultural Water Management, 98, 606–618.

Schickhoff, U., Singh, R.B., Mal, S., 2016. Climate change and dynamics of glaciers and vegetation in the Himalaya: an overview. In: Singh, R. B., Schikhoff, U., Mal, S., Eds) Climate change, glacier response, and vegetation dynamics in the Himalaya, Springer, Germany, 1–26.

Schwalbert, R.A., Amado, T., Corassa, G., Pott, L.P., Prasad, P.V.V., Ciampitti, I.A., 2020. Satellite-based soybean yield forecast: Integrating machine learning and weather data for improving crop yield prediction in southern Brazil. Agricultural and Forest Meteorology, 284, 107886.

Shao, Y., Campbell, J.B., Taff, G.N., Zheng, B.J., 2015. An analysis of cropland mask choice and ancillary data for annual corn yield forecasting using MODIS data. International Journal of Applied Earth Observation and Geoinformation, 38, 78–87.

Smith, B., Prentice, I.C., Sykes, M.T., 2001. Representation of vegetation dynamics in the modelling of terrestrial ecosystems: comparing two contrasting approaches within European climate space. Global Ecology and Biogeography, 10, 621–637.

Smith, B., Warlind, D., Arneth, A., Hickler, T., Leadley, P., Siltberg, J., Zaehle, S., 2014. Implications of incorporating N cycling and N limitations on primary production in an individual-based dynamic vegetation model. Biogeosciences, 11, 2027–2054.

Song, L., Guanter, L., Guan, K.Y., You, L.Z., Huete, A., Ju, W.M., Zhang, Y.G., 2018. Satellite sun-induced chlorophyll fluorescence detects early response of winter wheat to heat stress in the Indian Indo-Gangetic Plains. Global Change Biology, 24, 4023–4037.

Statistiska-Meddelanden., 2018. Harvest of cereals, legumes, oilseeds, potatoes and hay meadows 2018. Jordbruksverket [Online].

Stewart, J.I., & Hagan, E.M., 1973. Functions to predict effects of crop water deficits. J. Journal of the Irrigation and Drainage Division, 99 (4): 421–439.

Stoffelen, A., 1998. Toward the true near-surface wind speed: Error modeling and calibration using triple collocation. Journal of Geophysical Research: Oceans, 103(C4), 7755–7766.

Tadesse, T., Senay, G.B., Berhan, G., Regassa, T., Beyene, S., 2015. Evaluating a satellite-based seasonal evapotranspiration product and identifying its relationship with other satellite-derived products and crop yield: A case study for Ethiopia. International Journal of Applied Earth Observation and Geoinformation, 40, 39–54.

Talebizadeh, M., Moriasi, D., Gowda, P., Steiner, J.L., Tadesse, H.K., Nelson, A.M., Starks, P., 2018. Simultaneous calibration of evapotranspiration and crop yield in agronomic system modeling using the APEX model. Agricultural Water Management, 208, 299–306.

Tao, F.L., Rötter, R.P., Palosuo, T., Diaz-Ambrona, C.G.H., Mínguez, M.I., Semenov, M.A., Kersebaum, K.C., Nendel, C., Specka, X., Hoffmann, H., Ewert, F., Dambreville, A., Martre, P., Rodríguez, L., Ruiz-Ramos, M., Gaiser, T., Höhn, J.G., Salo, T., Ferrise, R., Bindi, M., Cammarano, D., Schulman, A.H., 2018. Contribution of crop model structure, parameters and climate projections to uncertainty in climate change impact assessments. Global Change Biology, 24, 1291–1307.

Taylor, K.E., Stouffer, R.J., Meehl, G.A., 2012. An overview of CMIP5 and the experiment design. Bulletin of the American Meteorological Society, 93, 485–498.

Tramontana, G., Jung, M., Schwalm, C.R., Ichii, K., Camps-Valls, G., Raduly, B., Reichstein, M., Arain, M.A., Cescatti, A., Kiely, G., Merbold, L., Serrano-Ortiz, P., Sickert, S., Wolf, S., Papale, D., 2016. Predicting carbon dioxide and energy fluxes across global FLUXNET sites with regression algorithms. Biogeosciences, 13(14), 4291–4313.

Tripathy, R., Chaudhari, K.N., Mukherjee, J., Ray, S.S., Patel, N.K., Panigrahy, S., Parihar, J.S., 2013. Forecasting wheat yield in Punjab state of India by combining crop simulation model WOFOST and remotely sensed inputs. Remote Sensing Letters, 4, 19–28.

Tubiello, F.N., Amthor, J.S., Boote, K.J., Donatelli, M., Easterling, W., Fischer, G., Gifford, R.M., Howden, M., Reilly, J., Rosenzweig, C., 2007. Crop response to elevated CO_2 and world food supply: A comment on “Food for Thought…” by Long et al., Science 312:1918–1921, 2006. European Journal of Agronomy, 26, 215–223.

Tucker, C.J., Holben, B.N., Elgin, J.H., Mcmurtrey, J.E., 1981. Remote-sensing of total dry-matter accumulation in winter-wheat. Remote Sensing of Environment, 11, 171–189.

Vazifedoust, M., van Dam, J.C., Bastiaanssen, W.G.M., Feddes, R.A., 2009. Assimilation of satellite data into agrohydrological models to improve crop yield forecasts. International Journal of Remote Sensing, 30, 2523–2545.

Waha, K., van Bussel, L.G.J., Muller, C., Bondeau, A., 2012. Climate-driven simulation of global crop sowing dates. Global Ecology and Biogeography, 21, 247–259.

Wang, E.L., He, D., Wang, J., Lilley, J.M., Christy, B., Hoffmann, M.P., O'Leary, G., Hatfield, J.L., Ledda, L., Deligios, P.A., Grant, B., Jing, Q., Nendel, C., Kage, H., Qian, B.D., Rezaei, E.E., Smith, W., Weymann, W., Ewert, F., 2022. How reliable are current crop models for simulating growth and seed yield of canola across global sites and under future climate change? Climatic Change, 20, 172.

Wardlow, B.D., & Egbert, S.L., 2008. Large-area crop mapping using time-series MODIS 250 m NDVI data: An assessment for the US Central Great Plains. Remote Sensing of Environment, 112, 1096–1116.

Webber, H., Ewert, F., Olesen, J.E., Müller, C., Fronzek, S., Ruane, A.C., Bourgault, M., Martre, P., Ababaei, B., Bindi, M., Ferrise, R., Finger, R., Fodor, N., Gabaldón-Leal, C., Gaiser, T., Jabloun, M., Kersebaum, K.C., Lizaso, J.I., Lorite, I.J., Manceau, L., Moriondo, M., Nendel, C., Rodríguez, A., Ruiz-Ramos, M., Semenov, M.A., Siebert, S., Stella, T., Stratonovitch, P., Trombi, G., Wallach, D., 2018. Diverging importance of drought stress for maize and winter wheat in Europe. Nature Communications, 9, 4249.

Wiréhn, L., 2018. Nordic agriculture under climate change: A systematic review of challenges, opportunities and adaptation strategies for crop production. Land Use Policy, 77, 63–74.

White, J.W., McMaster, G.S., Edmeades, G.O., 2004. Genomics and crop response to global change: what have we learned? Field Crops Research, 90, 165–169.

Wu, H., Xiang, J., Zhang, Y.P., Zhang, Y.K., Peng, S.B., Chen, H.Z., Zhu, D.F., 2018. Effects of post-anthesis nitrogen uptake and translocation on photosynthetic production and rice yield. Scientific Reports, 8, 12891.

Xiong, W., Holman, I., Conway, D., Lin, E., Li, Y., 2008. A crop model cross calibration for use in regional climate impacts studies. Ecological Modelling, 213, 365–380.

Xu, L., Chen, N.C., Zhang, X., Moradkhani, H., Zhang, C., Hu, C.L., 2021. In-situ and triple-collocation based evaluations of eight global root zone soil moisture products. Remote Sensing of Environment, 254, 112248.

Yang, Y., Anderson, M.C., Gao, F., Wardlow, B., Hain, C.R., Otkin, J.A., Alfieri, J., Yang, Y., Sun, L., Dulaney, W., 2018. Field-scale mapping of evaporative stress indicators of crop yield: An application over Mead, NE, USA. Remote Sensing of Environment, 210, 387–402.

Yang, Y., Anderson, M.C., Gao, F., Johnson, D.M., Yang, Y., Sun, L., Dulaney, W., Hain, C.R., Otkin, J.A., Prueger, J., Meyers, T.P., Bernacchi, C.J., Moore, C.E., 2021. Phenological corrections to a field-scale, ET-based crop stress indicator: An application to yield forecasting across the US Corn Belt. Remote Sensing of Environment, 257, 112337.

Yao, F.M., Tang, Y.J., Wang, P.J., Zhang, J.H., 2015. Estimation of maize yield by using a process-based model and remote sensing data in the Northeast China Plain. Physics and Chemistry of the Earth, 87–88, 142–152.

Yao, Y.J., Liang, S.L., Li, X.L., Chen, J.Q., Wang, K.C., Jia, K., Cheng, J., Jiang, B., Fisher, J.B., Mu, Q.Z., Grunwald, T., Bemhofer, C., Roupsard, O., 2015. A satellite-based hybrid algorithm to determine the Priestley-Taylor parameter for global terrestrial latent heat flux estimation across multiple biomes. Remote Sensing of Environment, 165, 216–233.

Yilmaz, M.T., Crow, W.T., Anderson, M.C., Hain, C., 2012. An objective methodology for merging satellite- and model-based soil moisture products. Water Resources Research, 48(11), W11502.

Zhang, X.B., Wan, H., Zwiers, F.W., Hegerl, G.C., Min, S.K., 2013. Attributing intensification of precipitation extremes to human influence. Geophysical Research Letters, 40, 5252–5257.

Zhang, Y.Q., Kong, D.D., Gan, R., Chiew, F.H.S., McVicar, T.R., Zhang, Q., Yang, Y.T., 2019. Coupled estimation of 500 m and 8-day resolution global evapotranspiration and gross primary production in 2002-2017. Remote Sensing of Environment, 222, 165–182.

Zhou, J.H., Crow, W.T., Wu, Z.Y., Dong, J.Z., He, H., Feng, H.H., 2021. A triple collocation-based 2D soil moisture merging methodology considering spatial and temporal non-stationary errors. Remote Sensing of Environment, 263, 112509.

Zhou, W.M., Liu, Y.J., Ata-Ul-Karim, S.T., Ge, Q.S., Li, X., Xiao, J.F., 2022. Integrating climate and satellite remote sensing data for predicting county-level wheat yield in China using machine learning methods. International Journal of Applied Earth Observation and Geoinformation, 111, 102861.